NON-LINEAR DYNAMIC ANALYSIS OF ANISOTROPIC CYLINDRICAL SHELLS CONTAINING A FLOWING FLUID

Aouni A. Lakis and André Laveau

Technical Report

No. EPM/RT-88/13

1988

Department of Mechanical Engineering

Ecole Polytechnique de Montréal

Campus de l'Université de Montréal

C.P. 6079 - Succ. "A" - Montréal

Québec, Canada H3C 3A7

TABLE OF CONTENTS

RESUME

Ce mémoire présente un modèle analytique pour prédire l'influence des non-linéarités associées à l'écoulememt sur le comportement dynamique de l'ensemble de la structure formée par la coque et le milieu fluide environnant. Sa formulation a nécessité l'emploi de deux opérateurs linéaires régissant respectivement l'équilibre de la coque et le potentiel des vitesses, d'une condition frontière d'imperméabilité linéaire, et d'une condition frontière dynamique non-linéaire.

Il s'agit d'une méthode hybride basée sur les théories des coques minces et des écoulements fluides irrotationnels non-visqueux et sur la méthode des éléments finis. Elle s'applique à des coques cylindriques minces anisotropes, non-uniformes et soumises à différentes conditions aux rives.

Les fonctions de déplacements de la paroi et de la colonne fluide sont dérivées respectivement des équations de Sanders et du champ de vitesse associé à la colonne. L'ensemble des matrices quantifiants leurs contributions relatives à l'équilibre sont déterminées par intégration analytique exacte.

La résolution des équations couplées a été effectuée pour un régime d'écoulement stagnant. Pour un régime avec écoulement, quelques adaptations analytiques sont proposées pour le ramener à l'analyse modale conventionnelle.

Les équations non-linéaires du mouvement sont solutionnées par une méthode numérique: le Runge-Kutta d'ordre quatre.

Les variations des fréquences sont alors déterminées en fonction de l'amplitude du mouvement. Les tendances des non-linéarités sont du type "softening".

ABSTRACT

This report presents an analytical model for predicting the influence of non-linearities associated with fluid flow on the dynamic behaviour of a structure consisting of shells and a surrounding fluid medium. The model requires use of two linear operators governing shell equilibrium and velocity potential, a linear boundary condition of impermeability and a non-linear dynamic boundary condition.

The model consists of a hybrid method, based on thin shell theory and the non-rotational flow of non-viscous fluids plus the finite element method. The method is applicable to non-uniform thin anisotropic cylinders subjected to different boundary conditions.

The displacement functions for the wall and liquid column are derived from Sanders' equations and from the velocity field associated with the column, respectively. The set of matrices describing their relative contributions to equilibrium is determined by exact analytical integration.

The coupled equations are solved for the no-flow problem. For cases where there is fluid flow, certain analytical modifications are proposed to bring the situation back to conventional modal analysis.

The non-linear equations of motion are solved by the 4th-order RUNGE-KUTTA numerical method.

The frequency variations are then determined with respect to the amplitude of the motion. The non-linearity trends are of the softening type.

REMERCIEMENTS

Ce document a pu être publié grâce à une subvention du Conseil de recherches en sciences et en génie du Canada (CRSNG) (Subv: no. A-8814) et le F.C.A.R. du Québec (Subv: no.EQ-1852).

Nous tenons à remercier Mme Danielle Therrien qui a dactylographié tous nos textes, modèles et formulaire.

Depôt legal, 2e trimestre 1986
Bibliothèque nationale du Québec
Bibliotheque nationale du Canada

Pour se procurer une copie de ce document, s'adresser aux:

Editions de l'Ecole Polytechnique de Montréal
Ecole Polytechnique de Montréal
Case postale 6079, Succursale "A"
Montréal (Québec) H3C 3A7
(514) 340-4000

Compter 0,10$ par page (arrondir au dollar le plus près) et aiouter 3,00$ (Canada) pour la couverture, les frais de poste et la manutention. Régler en dollars canadiens par chèque ou mandat-poste au nom de l'Ecole Polytechnique de Montréal. Nous n'honorerons que les commandes accompagnées d'un paiement, sauf s'il y a eu entente préalable dans le cas d'établissements d'enseignement, de sociétés ou d'organismes canadiens.

LIST OF SYMBOLS

$A_1; A_2$	Lamé parameters
A_j	constant in U equation
B_j	constant in V equation
C_j	constant in W equation
$\bar{C}_j$	vector {C} element
c	speed of sound in the fluid medium
D	membrane stiffness
E	Young's modulus
G	shear modulus of elasticity
J	number of boundary conditions applied
J_n	Bessel function of the first kind of order n
K	bending stiffness
L_i (i=1 @ 3)	linear differential operators associated with shell equilibrium
l	finite element length
$M_{11}, M_{22}, \bar{M}_{12}$	resultant moments
$M_{xx}, M_{\theta\theta}, \bar{M}_{x\theta}$	resultant couples in cylindrical coordinates
$\bar{\bar{M}}_1$	boundary couple value
m	number of axial half-waves
m_k	defined by relation (4.10)
N	number of finite elements

$N_{11}, N_{22}, \bar{N}_{12}$	resultant constraints
$N_{xx}, N_{\theta\theta}, \bar{N}_{x\theta}$	resultant constraints in cylindrical coordinates
n	number of circumferential modes
p	fluid pressure on wall
Q_1, Q_2	resultant shear constraints
Q_x, Q_θ	resultant shear constraints in cylindrical coordinates
R_1, R_2	radii of curvature of reference surface
R	average radius of cylindrical shell
R_N	Reynolds number
r	radial coordinate
t	wall thickness
$\bar{\bar{T}}_{12}$	resultant boundary shear
U, V, W	displacements: axial, tangential, radial
u_n, v_n, w_n	amplitudes of U,V,W associated with n^{th} circumferential mode number
U_x	flow velocity
V_r, V_x, V_θ	components of velocity field associated with the flow
x	cylinder generator coordinate
Y_n	Bessel function of the 2^{nd} kind of order n

$\frac{A}{t}$	non-dimensional vibration amplitude
$\frac{L}{R}$	structural slenderness
α_j, β_j	defined by relation (A-4,f)
Γ_{ij}	defined by relation (5.21)
$\varepsilon_{xx}, \varepsilon_{\theta\theta}, \bar{\varepsilon}_{x\theta}$	reference surface strain
ϖ_{ij}	defined by relation (5.21)
$k_{xx}, k_{\theta\theta}, \bar{k}_{x\theta}$	changes in curvature and torsion of reference surface
λ_j	complex root of characteristic equation
ν	Poisson's ratio
ρ_s	density of shell material
ρ_f	fluid density
ϕ	velocity potential
ω_L	linear natural angular frequency
ω_{NL}	non-linear natural angular frequency
Ω_{ij}	defined by relation (5.21)

LIST OF MATRICES

$[A]$	defined by relation (A-4,j)
$[A_f]$	defined by relation (4.16)
$[B]$	defined by relation (3.7)
$[BB']$	defined by relation (3.13)
$[c_f]$	fluid element damping matrix
$[c_f]_{NL}$	defined by relation (4.23)
$[D_f]$	defined by relation (4.20)
$[D_f]_{NL}$	defined by relation (4.26)
$[G_f]$	defined by relation (4.21)
$[G_f]_{NL}$	defined by relation (4.28)
$[GD_f]_{NL}$	defined by relation (4.27)
$[J]$	defined by relation (3.7)
$[J']$	defined by relation (3.14)
$[k_s]$	shell element stiffness matrix
$[k_f]$	fluid element stiffness matrix
$[k_f]_{NL}$	defined by relation (4.25)
$[kc_f]_{NL}$	defined by relation (4.24)
$[L]$	defined by relation (3.6)
$[L']$	defined by relation (3.14)
$[m_s]$	shell element mass matrix

$[m_f]$	fluid element mass matrix
$[N]$	shell nodal interpolation matrix
$[N_f]$	fluid nodal interpolation matrix compatible with shell matrix
$[P]$	matrix of elasticity
$[R']$	defined by relation (3.12)
$[S_f]$	defined by relation (4.19)
$[T]$	defined by relation (3.5)
$[X]$	defined by relation (3.6)
$\{q\}$	displacement vector in generalized coordinates
$\{\delta_i\}$	degrees of freedom vector at node i
$\{\Delta\}$	degrees of freedom vector for complete shell
$\{\varepsilon\}$	deformation vector
$\{\eta\}$	displacement vector in natural coordinates
$\{\sigma\}$	stress vector
$[\phi]$	eigenvector matrix

LIST OF TABLES

LIST OF FIGURES

CHAPTER I

INTRODUCTION

1.1 General

Shells are highly efficient elements of bearing structures. Their outstanding structural properties have been exploited since ancient times in shipbuilding, for example. Nowadays, thin shells are the basic structural components in aeronautical and aerospace manufacture.

Many theories have, therefore, focussed on the analysis of thin shells subjected to static or dynamic loads. It is generally agreed that vibration studies of this type of structure are classified according to factors such as: curvature, anisotropy, residual stresses, variation in thickness, large displacements, rotary inertia, effect of the environment, shape of the shell's edges and the type of boundary condition involved.

Most of these studies have involved linear analyses of thin shells both with and without interaction between the structure and the surrounding fluid medium. Results proved to be satisfactory where wall deflections are very small compared to the wall thickness. Hence, a knowledge of the dynamic characteristics of a shell containing a stationary or flowing fluid is of considerable interest to the engineer who is concerned with averting any destructive effects which could occur during industrial use of the shells.

In this type of investigation, the surrounding fluid medium is classified in terms of the following characteristics: type of flow, number of phases involved, the density, viscosity and compressibility of the fluid, and the free surface motion.

We owe the first attempt at an analytical formulation of the fluid medium's influence on the dynamic behaviour of an elastic shell to Rayleigh, in 1883. This was followed in 1909 by Nicolai. Since the end of World War II, this area of investigation has seen a large number of linear analyses of the free vibration characteristics of these structures ([1] to [7]). The characteristics of the damped

vibrations have been studied by Mizoguchi [8] and Lakis ([9], [25] to [30]).

In a large number of practical applications, a linear analysis is inadequate to predict the dynamic behaviour of structure/fluid systems. Analytical solution of the equations of motion for non-uniform thin shells is generally difficult, however, and only approximating methods are used. The fluid-shell wall interaction further complicates the analysis. Thus, studying the influence of non-linearity associated either with the strain-displacement relations for an empty shell [31], with the definition of flow or a combination of the two offers the investigator a multitude of avenues to explore for an enhanced understanding of the dynamic behaviour of these structures.

Among the approximating methods used for non-linear analysis of free vibration characteristics, we would mention the variational formulation [11], Galerkin's method ([12] and [13]) and the Rayleigh-Ritz method [14]. The true test of a method is whether it is able to determine the whole set of vibration frequencies and modes with the same precision and within reasonable processing time.

Galerkin's method does not meet this standard, in light of the loss in accuracy at the high shell frequencies. The Rayleigh-Ritz method satisfies the criterion by turning the vibration problem around into one involving solution of a symmetrical matrix system of eigenvalues.

There are a number of disadvantages associated with the Rayleigh-Ritz method, however: it requires a large number of terms to express the displacements; the accuracy provided for the displacement expressions is inconsistent with the accuracy associated with the energy and deformation expressions and, finally, there are concerns regarding the compatibility of the assumed displacement functions with the boundary conditions [15].

Reference [11] describes the free surface motion as governed by: a differential linear operator, a linear boundary condition and two other non-linear boundary conditions. Nevertheless, this model says nothing about dynamic interactions between the shell wall and the fluid.

References [12] and [13] report a dynamic stability study that was conducted using the non-linear equations in thin wall theory coupled with an equation giving a linear definition of the fluid velocity potential. The intrinsic drawback in this approach is that a shell of revolution is approximated by a set of curved plates.

Ramachandran's study [4] dealt with the effect of large deflections in a shell immersed in incompressible fluid. These non-linear displacement equations came from Donnell. Analysis of the results was deficient nevertheless due to insufficient rigour: he normalized the frequencies obtained by combining geometric non-linearities of the walls and the fluid interaction to results obtained with an empty shell.

1.2 Research Objectives

This report presents a general approach to the non-linear analysis of thin cylindrical anisotropic shells partially or completely filled with liquid under flow or no-flow conditions. It is a hybrid method, combining finite element and classical thin shell theory ([8], [25] to [32]). The finite element chosen was cylindrical (cf. Figure 5) and bounded by two circular nodes. There were four degrees of freedom at each node: axial, radial, circumferential displacement and rotation. The geometry of the

finite element made it possible to use Sanders' equations of motion [16] in their entirety to determine the displacement functions. This method therefore turns out to be more accurate than the usual polynomial functions that are chosen. Furthermore, the method is free of the disadvantages in the Rayleigh-Ritz method and satisfies the finite element method convergence criteria as well [24].

In the present research, we investigated the effect of non-linearities associated with the Bernoulli equation on the natural frequencies of an interactive fluid-shell system. The following experimental parameters were used in the analysis: circumferential mode, structural slenderness ratio, Reynolds number, vibration mode coupling and uncoupling and the effect of composite materials. We considered only the shell's breathing modes (i.e. where the longitudinal axis of the shell remains immobile during structure excitation).

The analytical solution was performed in two stages:

(1) Using the linear strain-displacement and stress-strain relationships which were inserted into the Sanders theory equations of equilibrium, we determined the displacement functions by solving the linear equation system. Next we determined the mass and stiffness matrices for a finite element, then assembled the matrices for the complete shell [24].

(2) The pressure exerted by the fluid was given by using a non-linear development of the Bernoulli equation. From our solution of the velocity potential equation we derived an expression of non-linear pressure as a function of 1) the nodal displacements of the fluid element, 2) the inertial, centrifugal and Coriolis forces and 3) a combination of non-linear effects. Through the usual finite element procedure, we obtained the linear mass, damping and stiffness matrices for the fluid [9] as well as the non-linear matrices for damping and stiffness and a combination of the two.

1.3 Outline of the Report

A brief overview of the contents of the eight chapters comprising this report is given below.

Chapter 2 contains a description of linear thin shell theory and a statement concerning the hypotheses underlying the research.

In Chapter 3, we give the three equations of motion with respect to the displacements and the elasticity matrix. Solving the characteristic equation gives the format of the displacement functions. We construct the mass and stiffness matrices for the shell.

Chapter 4 presents a development leading to a matrix formulation for linear mass, damping and stiffness and which gives non-linear effects for a fluid element.

Chapter 5 deals with the dynamic analysis of flow and no-flow conditions. For the latter case, we suggest a method for solving the coupled and non-linear equations of motion.

Chapter 6 discusses the numerical algorithm used in computing the different steps required in the model predicting the influence of Bernoulli related non-linearity on the natural frequencies of a fluid-shell system.

Chapter 7 reports the numerical results obtained and, finally, Chapter 8 contains the general conclusions of the study.

CHAPTER II

BASIC THEORY

2.1 Hypotheses

In order to study the equilibrium of a cylindrical shell including the membrane and bending effects on the reference surface, we used first-order Sanders equations [16]. These equations are based on Love's first approximation [17] and yield zero deformation for rigid-body motion, which is not true of other formulations.

The hypotheses for the analysis were as follows:

- The shell is made up of one or more layers of isotropic or orthotropic material.
- Displacements of the wall are sufficiently small to obtain geometric linearity.
- The terms for rotary inertia and shear deformation are neglected.
- Fluid characteristics: non-viscous
  incompressible

- Flow attributes: non-rotational
  potential
  frictionless
- The constants for internal pressure and surge pressure are ignored.

2.2 Method

The linear matrices were constructed using the procedure described in references [9] and [24]. The non-linear matrices were determined by development of the second-order Bernoulli equation.

Through modal analysis we transformed our equation of motion according to the axes of the natural coordinates. This analysis varies with the type of vibration encountered. Standard procedure was used for undamped free vibrations. For damped free vibrations, we propose a method which consists of considering all information contained in the eigenvalues and doing post-processing on the eigenvector matrix.

The coupled equations of motion were solved by means of the method used in reference [18].

CHAPTER III

MATRIX CONSTRUCTION: NO FLUID

3.1 Equations of Motion

Applying the virtual work principle to an infinitesimal element (cf. Figures 1 and 2) of a deformed average surface, we obtain the five equations of equilibrium describing the behaviour of a shell of arbitrary shape (Appendix A-1). We reduce them down to three equations by eliminating shear forces Q_x and Q_θ. In the absence of external forces, the equations of motion are as given in Appendix A-1 (d7 to d9).

Displacements of a point on the shell are related to the deformation vector by the strain-displacement relationships, which are given in detail in Appendix A-1 (d10 to d15). In its abbreviated form, the vector is written:

$$\{\varepsilon\} = \{\varepsilon_{xx}, \varepsilon_{\theta\theta}, 2\bar{\varepsilon}_{x\theta}, K_{xx}, K_{\theta\theta}, 2\bar{K}_{x\theta}\}^t \qquad (3.1)$$

where:
* ε_{xx}, $\varepsilon_{\theta\theta}$, $2\bar{\varepsilon}_{x\theta}$ are strains;
* K_{xx}, $K_{\theta\theta}$, $2\bar{K}_{x\theta}$ are changes in curvature and torsion;
* Subscripts x and θ designate the axial and circumferential coordinates.

The deformation vector is related to the stress vector by the stress-strain relationships.

$$\{\sigma\}=\{N_{xx},N_{\theta\theta},\bar{N}_{x\theta},M_{xx},M_{\theta\theta},\bar{M}_{x\theta}\}^{t}= [P]\ \{\varepsilon\} \qquad (3.2)$$

where: N_{xx}, $N_{\theta\theta}$, $\bar{N}_{x\theta}$, M_{xx}, $M_{\theta\theta}$, $\bar{M}_{x\theta}$ are resultant constraints.

Elements $p_{i\ j}$ in [P] describe the anisotropy of the shell.

Substituting (3.1) and (3.2) in (A-1, d7 to d9), we express the equilibrium equations in terms of the displacement functions [24]. Three differential linear operators are obtained (L_i, i = 1,2,3) and are given in full detail in Appendix A-2.

$$\begin{aligned} L_1\ (u,v,w,p_{ij}) &= 0 \\ L_2\ (u,v,w,p_{ij}) &= 0 \\ L_3\ (u,v,w,p_{ij}) &= 0 \end{aligned} \qquad (3.3)$$

where: u,v,w are the axial, tangential and radial displacements.

All values refer to the reference surface.

3.2 Elasticity Matrix

The elasticity matrix depends solely on the mechanical properties of the shell material. We will limit our analysis here to the anisotropic case of a shell of revolution commonly called orthotropy: the mechanical characteristics are invariant in rotation around a fixed axis.

For anisotropic material, [P] is generally written as [23]:

$$[P] = \begin{bmatrix} P_{11} & P_{12} & 0 & P_{14} & P_{15} & 0 \\ P_{21} & P_{22} & 0 & P_{24} & P_{25} & 0 \\ 0 & 0 & P_{33} & 0 & 0 & P_{36} \\ P_{41} & P_{42} & 0 & P_{44} & P_{45} & 0 \\ P_{51} & P_{52} & 0 & P_{54} & P_{55} & 0 \\ 0 & 0 & P_{36} & 0 & 0 & P_{66} \end{bmatrix} \qquad (3.4)$$

For a shell composed of a number of symmetric layers of iso- or orthotropic material arranged as in Figure 4, elements p_{ij} of [P] are expressed in the format given in Appendix A-3.

3.3 Displacement Functions

The shell of revolution is a deformable continuous medium with an infinite number of degrees of freedom. Its state of equilibrium is governed by equations (3.3). The original shell is partitioned into a number of finite elements having, therefore, a finite number of degrees of freedom. By carefully choosing the displacement functions, we transform our differential partial equations of equilibrium into a system of linear algebraic equations.

As displacements are periodic in the circumferential direction, we assume that the displacement functions can be expressed by expansion into a Fourier series [33].

$$\{u(x,\theta),w(x,\theta),v(x,\theta)\}^t = \sum_{n=1}^{\infty}[T(n,\theta)]\{u_n(x),w_n(x),v_n(x)\}^t \quad (3.5)$$

where n: number of circumferential modes

[T]: square diagonal matrix given in Appendix A-5.

The procedure for solving the (3.5) system of equations is described in Appendix A-4.

The resulting displacement becomes:

$$\{u,w,v\}^t = \sum_{n=0}^{\infty} [N] \begin{Bmatrix} \delta_i \\ \delta_j \end{Bmatrix} \tag{3.6}$$

$$\text{with } [N] = [T]\,[L]\,[X]\,[A^{-1}]$$

where [N]: 3 X 8 matrix
Exact nodal interpolation function defining displacement of point M.
[A], [L], [X]: matrices given in Appendix A-5
$\{\delta_i\}$: degrees of freedom associated with nodal displacements at boundary i.

3.4 Mass and Stiffness Matrices

The deformation vector $\{\epsilon\}$ (3.1) is expressed in terms of the nodal displacements (3.6).

$$\{\varepsilon\} = \sum_{n=0}^{\infty} [B] \begin{Bmatrix} \delta_i \\ \delta_j \end{Bmatrix} \tag{3.7}$$

where $[B] = [T^1]\,[J]\,[X]\,[A^{-1}]$

$$\text{with } [T^1] = \begin{bmatrix} [T] & 0 \\ 0 & [T] \end{bmatrix}$$

[J] is given in Appendix A-5.

The stress vector $\{\sigma\}$ (3.2) is also expressed in terms of the nodal displacements (3.6).

$$\{\sigma\} = [P]\,\{\varepsilon\}$$

$$\{\sigma\} = \sum_{n=0}^{\infty} [P]\,[B] \begin{Bmatrix} \delta_i \\ \delta_j \end{Bmatrix} \tag{3.8}$$

We have formulated our equilibrium equations and our strain-displacement and stress-strain relationships in terms of the nodal displacements. These displacements are determined by applying the Lagrangian equations to the discretized domain. Thus, the matrix format of the equations of motion is obtained as follows:

$$[m_s]\ \ddot{\{\delta\}} + [k_s]\ \{\delta\} = 0. \qquad (3.9)$$

where $[m_s]$: mass matrix for a finite element

$[k_s]$: stiffness matrix for a finite element
Both are 8 X 8.

These matrices are given by:

$$[m_s] = \rho_s t \int_{A_i} [N]^t\ [N]\ dA \qquad (3.10)$$

$$[k_s] = \int_{A_i} [B]^t [P]\ [B]\ dA$$

where $dA = R\,dx\,d\theta$

Using (3.6) and (3.7), we integrate (3.10) with respect to θ over the $[0,2\pi]$ interval, then to x over the $[0,1]$ interval, which gives us:

$$[m_s] = \pi R \rho_s t \; [A^{-1}]^t \; [R'] \; [A^{-1}]$$

$$[k_s] = \pi R \; [A^{-1}]^t \; [BB'] \; [A^{-1}] \qquad (3.11)$$

where the (p,q) term in [R'] is expressed by:

$$R'(p,q) = \begin{cases} \dfrac{L'(p,q)}{(\lambda_p+\lambda_q)} \left[e^{(\lambda_p+\lambda_q)1/R} - 1 \right] & \text{if } \lambda_p + \lambda_q \neq 0 \\ L'(p,q) \cdot 1 & \text{if } \lambda_p + \lambda_q = 0 \end{cases} \qquad (3.12)$$

and in [BB '] is given by:

$$BB'(p,q) = \begin{cases} \dfrac{J'(p,q)}{(\lambda_p+\lambda_q)} \left[e^{(\lambda_p+\lambda_q)1/R} - 1 \right] & \text{if } \lambda_p + \lambda_q \neq 0 \\ J'(p,q) \cdot 1 & \text{if } \lambda_p + \lambda_q = 0 \end{cases} \qquad (3.13)$$

where $[L'] = [L]^t \; [L]$

$[J'] = [J]^t \; [P] \; [J]$

l: finite element length
ρ_s: density of shell material

Inspecting relations (3.11) to (3.14), we can see that the mass and stiffness matrices for a finite shell element are therefore real and symmetric.

CHAPTER IV

ANALYTICAL FORMULATION: WITH FLUID

4.1 Dynamic Pressure

We are considering a cylindrical shell with a vertical generator axis. We shall use the procedure outlined in section 1.2 within the constraints of the hypotheses listed in section 2.1.

For ideal, frictionless flow, velocity potential [19] is governed by:

$$\nabla^2\phi = \frac{1}{c^2}\left[\vec{\nabla}\phi \cdot (\vec{\nabla}\phi \cdot \vec{\nabla})\,\vec{\nabla}\phi + \phi_{,tt} + 2\,\vec{\nabla}\phi \cdot \vec{\nabla}\phi_{,t}\right] \qquad (4.1)$$

where c: speed of sound in the fluid medium

ϕ: velocity potential

$$(\,)_{,t} : \frac{\partial(\,)}{\partial t}$$

Appendix B-1 gives the development of this 3rd-order non-linear equation in ϕ.

The linear form of the relation in (4.1) is expressed by:

$$\nabla^2\phi = \frac{1}{c^2}\left[\phi_{,tt} + 2\,U_x\phi_{,xt} + U_x^2\phi_{,xx}\right] \qquad (4.2)$$

Furthermore, for steady flow, the velocity potential must satisfy the Laplace. This relation is expressed according to a cylindrical coordinate reference point through:

$$\nabla^2 \phi = \frac{1}{r} (r\phi_{,r})_{,r} + \frac{\phi_{,\theta\theta}}{r^2} + \phi_{,xx} \qquad (4.3)$$

We define the velocity field associated with this flow by:

$$\begin{aligned} V_x &= U_x + \phi_{,x} \\ V_\theta &= \frac{\phi_{,\theta}}{r} \\ V_r &= \phi_{,r} \end{aligned} \qquad (4.4)$$

where U_x : Velocity associated with the flow rate by considering the fluid inviscid

A full definition of the flow requires two conditions applying to the shell-fluid interface. The impermeability condition ensures contact between the shell surface and the fluid. This should be:

$$V_r \Big|_{r=a} = \phi_{,r} \Big|_{r=a} = (\dot{W} + U_x W') \Big|_{r=a} \qquad (4.5)$$

The dynamic condition is given by the Bernoulli equation.

$$p_u = -\rho_{fu}\left(\phi_{,t} + U_{xu}\phi_{,x} + \frac{1}{2}\left[(\phi_{,x})^2 + \frac{(\phi_{,\theta})^2}{r^2} + (\phi_{,r})^2\right]\right)\Big|_{r=\xi} \qquad (4.6)$$

where u: subscript representing "in" or "out" as the case may be.

if u = i then $\xi = a_i = a - t/2$
if u = e then $\xi = a_e = a + t/2$

The development for the expression in (4.6) is given in Appendix B-2 (see also ref. [9]).

The differential operator is solved using the variable separation method. We first set the format for the radial displacement and velocity potential [9], as:

$$W_k = C_k e^{i(n\theta + \lambda_k \frac{x}{a} + wt)} \qquad (4.7)$$

$$\phi = \sum_{k=1}^{8} \phi_k = \sum_{k=1}^{8} R_k(r) \quad S_k(\theta,x,t) \qquad (4.8)$$

where λ_{mn} : kth root of the characteristic equation

ω_{mn} : natural angular frequency

Applying the impermeability condition, we determine $S_k(\theta,x,t)$ explicitly. If we set relations (4.2) and (4.3) as equal, we will obtain the ordinary homogeneous differential Bessel equation:

$$r^2 \frac{d^2 R_k(r)}{d r^2} + r \frac{dR_k(r)}{d r} + R_k(r) \left[i^2 m_k^2 r^2 - n^2 \right] = 0 \qquad (4.9)$$

$$\text{where } m_k = \left(\frac{\lambda_k}{a_u} \right)^2 - \frac{1}{c^2} \left\{ w + U_{xu} \frac{\lambda_k}{a_u} \right\}^2 \qquad (4.10)$$

We carry the Bessel equation solution back into (4.8) to obtain the final expression of the velocity potential evaluated at the cylinder wall.

$$\phi_u(r,\theta,x,t)_k = a_u Z_{k\,u}(i m_k a_u) \left[W_{k,t} + U_{xu} W_{k,x} \right] \qquad (4.11)$$

$$\text{where } Z_{k\,u}(i m_k a_u) = \frac{1}{n - i m_k a_u \dfrac{J_{n+1}(i m_k a_u)}{J_n(i m_k a_u)}} \qquad \text{if } u = i \qquad (4.12)$$

$$Z_{k\,u}(i m_k a_u) = \frac{1}{n - i m_k a_u \dfrac{Y_{n+1}(i m_k a_u)}{Y_n(i m_k a_u)}} \qquad \text{if } u = e$$

Substituting (4.11) into the non-linear boundary condition expression (4.6), we obtain the equation for pressure on the cylinder wall. It is useful to partition total pressure into its linear and non-linear terms:

$$p = \{ p_{in} - p_{out} \}_L + \{ p_{in} - p_{out} \}_{NL} \tag{4.13}$$

where $$p_{u\,L} = -\rho_{fu} \sum_{p=1}^{8} a_u Z_{p\,u} [W_{p,tt} + 2U_{xu} W_{p,xt} + U_{xu}^2 W_{p,xx}] \tag{4.14}$$

$$p_{u\,NL} = -\frac{\rho_{fu}}{2} \sum_{p=1}^{8} \sum_{q=1}^{8} \{ \alpha_p \alpha_q [W_{p,xt} W_{q,xt} + 2U_{xu} W_{p,xx} W_{q,xt} + U_{xu}^2 W_{p,xx} W_{q,xx}] + \beta_p \beta_q [W_{p,t} W_{q,t} + 2U_{xu} W_{p,t} W_{q,x} + U_{xu}^2 W_{p,x} W_{q,x}] \} \tag{4.15}$$

where $\alpha_p = a_u Z_{p\,u}$ $\quad \beta_p = 1 - nZ_{p\,u}$

$\beta_q = 1 + nZ_{q\,u}$

4.2 Linear Matrices for the Fluid Column

We introduce the nodal interpolation functions for the fluid which are compatible with the functions for the shell (3.6) into the dynamic pressure expression in (4.14) and execute a series of intermediate matrix operations made necessary by our choice of method. The mass, damping and stiffness matrices for the fluid are obtained by evaluating the following integral [9]:

$$\int_A [N_F]^t \{ p_L \} \, dA$$

Finally, we have:

$$[m_f] = [A_f^{-1}]^t [S_f] [A_f^{-1}] \tag{4.16}$$

$$[c_f] = [A_f^{-1}]^t [D_f] [A_f^{-1}] \tag{4.17}$$

$$[k_f] = [A_f^{-1}]^t [G_f] [A_f^{-1}] \tag{4.18}$$

where $S_f(p,q) = \pi [-\delta_i \gamma_i^2 Z_{q\ i} I_{pq\ i} + \delta_e \gamma_e^2 Z_{q\ e} I_{pq\ e}]$ (4.19)

$$D_f(p,q) = 2i\lambda_q \pi [-\delta_i \gamma_i \bar{U}_i Z_{q\ i} I_{pq\ i} + \delta_e \gamma_e \bar{U}_e Z_{q\ e} I_{pq\ e}] \tag{4.20}$$

$$G_f(p,q) = -\lambda_q^2 \pi [-\delta_i \bar{U}_i^2 Z_{q\ i} I_{pq\ i} + \delta_e \bar{U}_e^2 Z_{q\ e} I_{pq\ e}] \tag{4.21}$$

and $p, q = 1, \ldots 8$

In equations (4.19) to (4.21) we define the following non-dimensional quantities:

$$\delta_u = \frac{a_u \rho_{fu}}{t_1 \rho_1} \qquad U_o^2 = \frac{p(1,1,1)}{\rho_1 t_1}$$

$$\bar{U}_u = \frac{U_{xu}}{U_o} \qquad \gamma_u = \frac{a_u}{r_1}$$

where ρ_1 : density

t : thickness of the first finite element of the shell

r : radius

$p(1,1,1)$: 1st element of [P]

$$I_{pq\,u} = \frac{e^{i(\lambda_p + \lambda_q)\frac{l_j}{a_u}} - 1}{i(\lambda_p + \lambda_q)} \qquad \text{if } \lambda_p + \lambda_q \neq 0$$

$$I_{pq\,u} = \frac{l_j - l_i}{a_u} \qquad \text{if } \lambda_p + \lambda_q = 0 \qquad (4.22)$$

4.3 Development of the Non-linear Matrices

We use the procedure outlined in the previous section, ignoring the cross products in the non-linear dynamic pressure expression (4.15). We obtain the following matrices for the non-linear effects:

$$[c_f]_{NL} = [A_f^{-1}]^t [D_f]_{NL} [A_f^{-1}] \tag{4.23}$$

$$[kc_f]_{NL} = [A_f^{-1}]^t [GD_f]_{NL} [A_f^{-1}] \tag{4.24}$$

$$[k_f]_{NL} = [A_f^{-1}]^t [G_f]_{NL} [A_f^{-1}] \tag{4.25}$$

where:

$$D_{f_{NL}}(p,q) = \frac{e^{6\pi in} - 1}{6in} \{ \delta_i \gamma_i J_{pq\ i} [Z^2_{q\ i} [n^2 + \lambda_q^2] - 1]$$

$$- \delta_e \gamma_e J_{pq\ e} [Z^2_{q\ e} [n^2 + \lambda_q^2] - 1] \} \tag{4.26}$$

$$GD_{f_{NL}}(p,q) = \frac{(e^{6\pi in} - 1)\ \lambda_{q\,i}}{3in} \{ \delta_i \bar{U}_i J_{pq\ i} [Z^2_{q\ i} [n^2 + \lambda_q^2] - 1]$$

$$- \delta_e \bar{U}_e J_{pq\ e} [Z^2_{q\ e} [n^2 + \lambda_q^2] - 1] \tag{4.27}$$

$$G_{f_{NL}}(p,q) = \frac{-(e^{6\pi in} - 1)\ \lambda_q^2}{6in} [\frac{\delta_i \bar{U}_i^2}{\gamma_i} J_{pq\ i} [Z^2_{q\ i} [n^2 + \lambda_q^2] - 1]$$

$$- \frac{\delta_e \bar{U}_e^2}{\gamma_e} J_{pq\ e} [Z^2_{q\ e} [n^2 + \lambda_q^2] - 1] \} \tag{4.28}$$

$$\text{where: } J_{pq\,u} = \frac{e^{i(\lambda_p + 2\lambda_q)\frac{l_j}{a_u}} - 1}{i(\lambda_p + 2\lambda_q)} \qquad \text{if } \lambda_p + 2\lambda_q \neq 0 \tag{4.29}$$

$$J_{pq\,u} = \frac{l_j - l_i}{a_u} \qquad \text{if } \lambda_p + 2\lambda_q = 0$$

CHAPTER V

ANALYSIS OF FREE VIBRATIONS

5.1 Global Matrices

The motion of a shell element interacting with a fluid column is governed by the equations of motion in generalized coordinates.

$$[[m]_s-[m]_f]_L\{\ddot{\delta}\}-[c]_L\{\dot{\delta}\}+[[k]_s-[k]_f]_L\{\delta\}-[c]_{NL}\{\dot{\delta}\}^2-[kc]_{NL}\{\delta\dot{\delta}\}-[k]_{NL}\{\delta\}^2=\{0\}$$

where subscripts s and f refer to the shell and fluid, respectively.

$\{\Delta\}$ is the degrees of freedom vector for the total nodes, and total structure motion is governed by an analogous equation which we shall write:

$$[[M]_S-[M]_F]_L\{\ddot{\Delta}\}-[C]_L\{\dot{\Delta}\}+[[K]_S-[K]_F]_L\{\Delta\}-[C]_{NL}\{\dot{\Delta}\}^2-[KC]_{NL}\{\Delta\dot{\Delta}\}-[K]_{NL}\{\Delta\}^2=\{0\} \quad (5.2)$$

These global matrices are obtained by assembling the element matrices. The assembly operation must satisfy two conditions however [20]:

- Continuity of nodal displacements at the boundary between two adjacent elements, such that:

$$\{\delta_{i+1}\} = \{\delta_j\}$$

- External forces and moments applied at a given node must be equal, respectively, to the internal forces and moments, such that:

$$\{f\}^e = \{f_j\} + \{f_{i+1}\}$$

Assembling the matrices is done using the overlay method [24], as illustrated in Figure 6. The global matrices are square, of order 4(N+1), where N is the number of finite elements.

5.2 Equations of Motion

After the boundary conditions are applied, these matrices are reduced to square matrices of order 4(N+1)-J.

where J: number of restrictions imposed.

To abbreviate the expression, we set:

$$[M_T] = [[M]-[M]] \text{ et } [K_T] = [[K]-[K]]$$
$$\qquad S \quad F \qquad\qquad S \quad F$$
$$\qquad\quad L \qquad\qquad\quad L$$

$$[M_T]\{\ddot{\Delta}\}-[C_{LF}]\{\dot{\Delta}\}+[K_T]\{\Delta\}-[C]\{\dot{\Delta}\}-[KC]\{\Delta\dot{\Delta}\}-[K]\{\Delta^2\}=\{0\} \quad (5.3)$$
$$\qquad\quad F \qquad\quad F \qquad\quad F \qquad\quad F$$

where r means reduced.

Let us set $\{ \Delta^{r} \} = [\phi] \{\eta\}$ (5.4)

where $[\phi]$: : square eigenvector matrix in the symmetric linear matrix system

$\{\eta\}$, $\{ \Delta^{r} \}$: displacement vectors expressed as natural and generalized coordinates, respectively.

$[\ ^{r}\ ]$: ... matrix ... generalized coordinates

We first substitute expression (5.4) into (5.3), then multiply (5.3) by $[\phi]^{t}$ to obtain, finally:

$$[M^{D}_{T}]\{\ddot{\eta}\}-[C^{D}_{L}]\{\dot{\eta}\}+[K^{D}_{T}]\{\eta\}-[\phi][C^{t}_{NL}][\phi^{2}]\{\dot{\eta}^{2}\}$$

$$-[\phi][KC^{t}_{NL}][\phi^{2}]\{\eta\dot{\eta}\}-[\phi][K^{t}_{NL}][\phi^{2}]\{\eta^{2}\} = \{0\} \quad (5.5)$$

with $[M^{D}] = [\phi]^{t} [M]_{T} [\phi]$

$[C^{D}] = [\phi]^{t} [C]_{F} [\phi]$

$[K^{D}] = [\phi]^{t} [K]_{T} [\phi]$

where D stands for diagonal

$[\ ^{D}\ ]$: ... matrix ... natural coordinates

The matrices quantifying the fluid column contribution to the matrix equations of motion are non-symmetric. To facilitate analysis, therefore, we consider only the symmetric portion of the matrices. We will be seeing later on that this simplification is justified.

5.21 No-flow Conditions

Under stagnant conditions, equation (5.2) reduces to:

$$[M]_T \{\ddot{\Delta}\} + [K] \{\Delta\} - [C]_F \{\dot{\Delta}^2\} = \{0\} \qquad (5.6)$$

First we solve for the linear case to obtain the 4*(N+1)-J eigenvalues and eigenvectors. With this eigenvector matrix, we then develop the coupled equations of motions in natural coordinates.

5.22 Flow Conditions

As mentioned in section 2.2, we make some modifications to the procedure described above.

Due to the presence of a non-proportional damper, we reduce the 2nd-order linear system to a 1st-order system. We again consider only the symmetric portions of the fluid matrices, as given in the equation:

$$[M]\{\ddot{q}\} + [C]\{\dot{q}\} + [K]\{q\} = \{0\} \qquad (5.7)$$

which may be represented by the following form [21]:

$$[A]\{\dot{y}\} + [B]\{y\} = \{0\} \qquad (5.8)$$

where: $[A] = \begin{bmatrix} 0 & [M] \\ [M] & [C] \end{bmatrix}$

$$[B] = \begin{bmatrix} -[M] & 0 \\ 0 & [K] \end{bmatrix}$$

$$\{y\} = \begin{Bmatrix} \{\dot{q}\} \\ \{q\} \end{Bmatrix}$$

We assume the form of the homogeneous solution to be:

$$\{y(t)\} = e^{\lambda t}\{\Psi\} \qquad (5.9)$$

Relation (5.7) becomes:

$$\lambda [A]\{\Psi\} = -[B]\{\Psi\} \qquad (5.10)$$

From the solution of (5.10), we obtain a series of 2n eigenvalues and 2n eigenvectors. For each given eigenvalue, λ_n, the corresponding eigenvectors are developed as follows:

$$\{\Psi_n\} = \begin{bmatrix} \lambda\{\phi_n\} \\ \{\phi_n\} \end{bmatrix} \qquad n = 1, 2, \ldots N \qquad (5.11)$$

where N: number of degrees of freedom

The eigenvalues are complex and always occur in conjugate pairs.

The dimensional incompatibility between the eigenvector matrices defined in (5.4) and (5.11) and the absence of any weighted orthogonal relationships between the [M], [C] and [K] matrices in (5.7) are difficulties which have to be overcome.

We attempt to determine the m_{ii}, c_{ii} and k_{ii} for each of the uncoupled equations of motion. To this end we have two pieces of information (concerning the state of the damped system) for each eigenvalue pair.

We have:

$$\lambda_n = \alpha + i\beta \qquad (5.12)$$

According to (5.9) and (5.12), we also have:

$$y_n(t) = \psi_n e^{\lambda_n t} = \psi_n e^{\alpha_n t} e^{i\beta_n t} \qquad (5.13)$$

Now, for a damped system, the displacement is defined by [21]:

$$y_n(t) = Y_o e^{-\xi w_n t} e^{i w_d t} \qquad (5.14)$$

where γ_o : initial amplitude

ξ : critical damping coefficient

w_n : natural angular frequency

w_d : damped angular frequency

We then, by analogy, associate the terms in relations (5.13) and (5.14) to find our unknowns. Finally, we obtain:

$$k_{nn} = (\alpha_n^2 + \beta_n^2) m_{nn} \qquad (5.15)$$

$$c_{nn} = 2\,\alpha_n\, m_{nn} \qquad (5.16)$$

The m_{nn} are taken from the orthogonal relation:

$$\{\Psi\}^t [B] \{\Psi\} = 0 \qquad (5.17)$$

The first n diagonal terms of the resulting matrix are the n elements of diagonal [M].

The eigenvector matrix is constructed by selecting and assembling side-by-side the n column vectors $\{\phi_N\}$ in (5.11) associated with each pair of eigenvalues λ_N . With this $[\phi]$, we then go on to couple the motion equations in natural coordinates (5.5).

5.3 Solving the Coupled Equations

During the modal analysis, we have to consider coupling between the different modes since products of the form $[\phi]^t\,[M]\,[\phi^2]$ do not generally give diagonal matrices.

A typical system equation therefore would be of the form:

$$m_{ii}\,\ddot{\eta}_i - c_{ii}\,\dot{\eta}_i + k_{ii}\eta_i - \sum_{j=1}^{NREDUC}\{C_{ij}\dot{\eta}_i\dot{\eta}_j + KC_{ij}\eta_i\dot{\eta}_j + K_{ij}\eta_i\eta_j\}=0 \qquad (5.18)$$

Let us set:

$$\eta_i(\tau) = A_i\,f_i(\tau) \qquad (5.19)$$

which satisfies the initial conditions

$$f_i(0) = 1 \qquad \text{and} \qquad \dot{f}_i(0) = 0 \qquad (5.20)$$

where A_i : vibration amplitude

Relation (5.18), after simplifying by A_i and dividing by m_{ii}, becomes:

$$\ddot{f}_i - \frac{1}{\tau_i}\,\dot{f}_i + \omega_i^2\,f_i - \sum_{j}^{NREDUC}\left(\frac{A_i}{t}\right)\{\Gamma_{ij}\dot{f}_i\dot{f}_j + \varpi_{ij}f_i\dot{f}_j + \Omega_{ij}f_if_j\} = 0 \qquad (5.21)$$

where $\omega_i^2 = \frac{k_{ii}}{m_{ii}}$ $\qquad \frac{1}{\tau_i} = \frac{c_{ii}}{m_{ii}}$

$$\Gamma_{ij} = \frac{C_{ij}^{(NL)}\, t}{m_{ii}} \qquad \text{æ}_{ij} = \frac{KC_{ij}^{(NL)}\, t}{m_{ii}}$$

$$\Omega_{ij} = \frac{K_{ij}^{(NL)}\, t}{m_{ii}}$$

t: shell thickness

If, however, we ignore non-linear coupling between the natural coordinates, equation (5.21) will take the form:

$$\ddot{f}_i - \frac{1}{\tau_i}\dot{f}_i + \omega_i f_i - \left(\frac{A_i}{t}\right)\{\Gamma_{ii}\dot{f}_i^2 + \text{æ}_{ii}\dot{f}f_i + \Omega_{ii}f_i^2\} = 0 \qquad (5.22)$$

The solution $f_i(\tau)$ of these ordinary non-linear differential equations which satisfies the initial conditions (5.20) is approximated numerically by a fourth-order Runge-Kutta. The linear and non-linear natural angular frequencies are evaluated by a systematic search for the $f_i(\tau)$ roots as a function of time. The ω_{NL}/ω_L ratio is expressed as a function of non-dimensional ratio A_i/t.

CHAPTER VI

THE ALGORITHM

Numerical application of the analytic formulations described in this report required four computer programs. These programs were written in Fortran versions IV and V and were run on a CDC CYBER 855 [31].

The initial cylindrical shell was subdivided into a sufficient number of finite elements to ensure convergence with the method. For each finite element, the calculations were divided into three stages: the first relates to the linearity of the strain-displacement relationships, the other two to the linearity and non-linearity, respectively, associated with the Bernoulli equation.

Execution of the algorithm required input of the following information:

i) number of finite elements

ii) geometry of each finite element: length, radius, thickness

iii) mechanical properties of each distinct shell section: Young's modulus, Poisson's ratio and density

iv) boundary conditions

v) characteristics of the fluid column: density, flow conditions

vi) number of circumferential modes

Below is a list of the main steps in the calculations that were done for each n harmonic.

The procedure the algorithm follows involves determining:

a) for each finite shell element:

i) the characteristic equation coefficients as given in Appendix A-6

ii) the 8 λ_i roots of the characteristic equation. They are determined by the Laguerre method with the help of IMSL's ZPOLR subroutine.

iii) coefficients α_i and β_i defined by the relations given in Appendix A-4

iv) matrix [A] defined in Appendix A-4 and its inverse, by the LINV2F subroutine from IMSL

v) matrices [R'] and [BB'] defined by (3.12) and (3.13)

vi) the elemental mass [m] and stiffness [k] matrices defined by (3.11)

b) for each finite fluid column element:

i) the $[A_F]$ matrix compatible with the matrix defined in Appendix A-5 and its inverse, by IMSL's LEQT2DC subroutine

ii) matrices $[S_{F\ L}]$, $[D_{F\ L}]$, $[G_{F\ L}]$ and $[D_{F\ NL}]$, $[GD_{F\ NL}]$, $[G_{F\ NL}]$ given by the equation systems in (4.19) to (4.21) and (4.26 to (4.28), respectively

iii) the elemental mass $[m_F]$, damping $[c_F]$, and stiffness $[k_F]$ matrices plus the second-order non-linear effects $[C_F]$, $[KC_F]$, $[K_F]$ given, respectively, by (4.16) to (4.18) and (4.23) to (4.25)

c) the global matrices (corresponding to the matrices defined above) for the complete shell, to be assembled

d) the matrices reduced by application of the boundary conditions

e) the mass and stiffness matrices of the shell-fluid system, by overlaying the corresponding matrices

f) the natural vibration frequencies and the main modes associated with them. The EIGZF program from IMSL is used for that purpose [9].

g) the diagonal terms in the mass, damping and stiffness matrices, using the methods described in section 5.2

h) products of the form $[\phi^t]\,[A]\,[\phi^2]$ from system (5.5)

i) the influence of non-linearity in the flow definition on the natural frequencies of equation system (5.21). the RUNGE program is used to quantify the influence.

CHAPTER VII

CALCULATIONS AND DISCUSSION

7.1 Introduction

This chapter will be describing application of the new method proposed to a number of cases.

First, calculations were done to demonstrate the validity of the simplifying hypothesis we described in (5.21). Next, we conducted a systematic investigation into the influence of the non-linearities associated with the Bernoulli equation by considering the experimental parameters listed in section 1.2. Finally, we will briefly discuss the stability problem inherent in the dynamic behaviour of the equation system studied.

7.2 Validitation of the Simplifying Hypothesis

Development of the analytical model required an additional hypothesis. Indeed, with the present state of our knowledge, we are unable to apply the orthogonality properties of the modal vectors to a general eigenvalue problem ([21], [22]). We are thus simplifying the parameters and limiting our dynamic analysis strictly to consideration of shell-fluid systems that lead to a symmetric matrix system of eigenvalues.

This simplifying hypothesis is validated if the resultant eigenvalues substantially approach the original system. Tables 1 to 4 show the variance between the eigenvalues in the original and simplified systems, corresponding to cases of damped and undamped free vibration. A trend was observed toward minimum variance at the extremal modes and maximum variance (15% and 19.5% for a damped and undamped case, respectively) at the median modes.

The simplification therefore seems to be right since it describes both systems as having comparable dynamic behaviour.

7.3 Analysis of Results

We used four cylindrical shell models to investigate the influence of a fluid medium. The shell had the properties given in reference [13].

$E = 20.685 \times 10^3$ MPa (steel)
$\nu = 0.29$
$R = 193.675$ mm
$t = 1.29117$ mm
$\rho_{shell} = 7.8125 \times 10^3$ Kg / m^3
$\rho_{water} = 1.0000 \times 10^3$ Kg / m^3

$\} \frac{R}{t} = 150$

$\} \frac{\rho_{water}}{\rho_{shell}} = 0.128$

The boundary conditions were for a shell simply supported at both ends, such that V=W=0.

The parameters of the investigation took the following values:

- n = 3 and 6 corresponding to the 3rd and 6th circumferential vibration mode
- structural slenderness ratio
  L/R = 3 and 6
- Reynolds number
  R_N = 0 (undamped vibration)
  R_N = 1.0E+06 and 2.0E+06 (damped vibration)

Young's modulus of elasticity

E_{steel} and $E_{steel}/100$

All the graphs illustrating our analysis may be found in Appendix I. A synopsis of their overall characteristics is nevertheless given in Table 5.

It can be seen, first of all, that the variation in frequency ratio (W_{NL}/W_L) decreases with increases in the non-dimensional end mass ratio. There does therefore appear to be a generalized form linear trend of the softening type. In addition, the earliest occurrences of sensitivity to this non-linearity are associated with a clustering of the first and last axial modes for cases of damped and undamped vibrations, respectively.

We shall now describe the parameter variables in terms of their relative impact on frequency ratio variations. In all cases, uncoupling the equations of motion produces more pronounced variation than coupling. For the reason mentioned in section 5.3, solution of the coupled equations provides a better assessment of the relative weight of the effects analyzed. The variation is low to moderate and moderate to high, respectively, for no-flow and flowing fluid columns. Finally, their relative impact on the other

parameters of our study, in descending order, is: the circumferential vibration mode, composite material effect and structural slenderness ratio.

A glance at the synopsis in Table 5 reveals the large amplitudes required to obtain any tangible effect. An amplitude of this magnitude corresponds to a pump discharge pulse or "water hammer" effect!

It would be of interest nevertheless to explore the possible influence of composite materials further, since the order of magnitude for the non-dimensional amplitude ratio is the closest to unity.

There are two other avenues of investigation which hold out inviting prospects - the boundary condition and compressibility effects. Common in the aviation industry is a particular structure that falls perfectly into our analytical model: the jet engine nozzle, which is a clamped-free structure. It also involves the possibility of coupling occurring between the modes associated with floating instabilities and the non-linearity studied when Mach number verges on 0.30.

Our investigation to date has thus confirmed the hypothesis stating that the influence of Bernoulli equation non-linearity on the dynamic behaviour of the shell-fluid structure is negligible.

7.4 Numerical Stability

We had some difficulty in stabilizing solution of the non-linear equations of motion under one particular condition. This condition related to the magnitude of the contribution by the non-linear effects to system inertia. Furthermore, damped structures also present greater numerical stability than undamped structures.

The instabilities were characterized either by oscillations whose frequencies varied substantially through time or by an inconsistency between the frequency and rate of these oscillations around the balanced position. This occurred right from the initial pulse.

We adopted a convergence criterion which would keep us within the realm of stability. The criterion involved making sure that the solution would repeat by considering a frequency response acceptable if it fell within a band under 1% of its nominal value.

7.5 Processing Time

The computer program was run on a Cyber 855 computer in the University of Montreal Computer Centre. This CDC product allows for an internal 60-bit single-precision representation of numbers in floating-point mode (48 bits for the mantissa, 11 for the exponent and 1 for the sign).

In the following paragraph is the running time and memory required for the case described below:

Shell model No. 1 subdivided into 5 finite elements with a fluid column velocity corresponding to R_N = 1.0 E+06.

CPU time	:	100 sec.
Memory space	:	134000 bytes
Cost	:	$35.00 (Cdn)

We would mention however that the program was designed to ensure compatibility with existing programming. Structured programming of the master program and the option of dynamic memory allocation are improvements that could be considered for a more flexible and higher-performance machine code.

CHAPTER VIII

CONCLUSION

For the purposes of our analysis, a method based on Sanders' thin shell equations, equations for non-rotational and frictionless fluid flow and on the finite element method as its basic skeleton was developed. The method predicts the influence of non-linearity associated with the flow definition on the dynamic behaviour of vertical cylindrical shells partially or completely filled with a stagnant or flowing liquid.

The finite element was cylindrical and geometrically axisymmetric. The displacement functions were therefore derived from the equations of motion for the shell. The mass and stiffness matrices were determined by exact analytical integration. The displacement functions for the fluid column were derived from the velocity field associated with the column and from the non-linear impermeability and dynamic conditions applied to the shell-fluid interface. The matrices for the fluid column contribution were determined in a manner similar to the matrices for the shell wall.

Conventional modal analysis was used to treat a shell with undamped free vibrations and vibrations damped with a non-proportional damper. This latter vibration case required therefore a simplifying hypothesis which proved justified as well as a few analytical modifications.

The non-linear equations of motion expressed in natural coordinates were solved using a numerical time-based integral method: the fourth-order Runge-Kutta.

This area of investigation is still wide open and there is a dearth of literature on the subject. We are unable, therefore, at this stage in our research to confirm whether, in the context of a dynamic analysis, we are justified in completely neglecting the influence of the non-linear boundary condition at the shell-fluid interface.

The present theory was formulated and applied to straight cylindrical shells with circular sections. It can however be used to analyze a shell of revolution with arbitrary curvature by proper assembly of the cylindrical, conical or spherical elements to approximate the geometry desired.

It would be interesting to apply the method developed to investigations of forced vibrations in a cylindrical shell subjected to dynamic loads. It would also be interesting to include phenomena of flotation and buckling instability in our analysis.

Finally, the logical extension to the work of our group would be to investigate the effect of geometric non-linearities of the walls on the dynamic behaviour of the shell-fluid interaction.

REFERENCES

[1] Junger, M.C., "Dynamic behavior of reinforced cylindrical shells in a vacuum and in a fluid". J. Appl. Mech., vol. 21, no. 1, 1954, pp. 35-41.

[2] Berry, J.G.; Reissner, E., "The effect of an internal compressible fluid column on the breathing vibrations of a thin pressurized cylindrical shell". J. Aerospace Sci., vol. 25, no. 5, May 1958, pp. 288-294.

[3] Lindholm, U.S.; Kana, D.D.; Abramson, H.N., "Breathing vibrations of a circular cylindrical shell with an internal liquid". J. Aerospace Sci., vol. 29, Sept. 1962, pp. 1052-1059.

[4] Lindholm, U.S.; Chu, W.H.; Kana, D.D.; Abramson, H.N., "Bending vibrations of a circular cylindrical shell with an internal liquid having a free surface". AIAA J., vol. 1, no. 9, Sept. 1963, pp. 2092-2099.

[5] Abramson, H.N., "The dynamic behavior of liquids in moving containers". NASA SP-106, 1966.

[6] Rabinovich, B.I., "Equations of transverse vibrations of fluid-filled shells". NASA TT F-216.

[7] Jain, R.K., "Vibration of fluid-filled, orthotropic cylindrical shells". J. of Sound and Vibration, vol. 37, no.3, 1974, pp. 379-388.

[8] Mizoguchi, Kodi, "Vibration of a cylindrical shell containing a flowing fluid". JSME, vol. 10, no. 37, 1967, pp. 59-67.

[9] Lakis, A.A., "Effects of fluid pressures on the vibration characteristics of cylindrical vessel". Second International Conference on Pressure Surges, Sept. 1976, paper J1.

[10] Leissa, A.W., "Vibration of shells". NASA SP-288.

[11] Admire, J.R., "Nonlinear fluid oscillations in a partially filled axisymmetric container of general shape". NASA TN D-5808, June 1970.

[12] Obraztsova, E.I., "Nonlinear parametric oscillations of cylindrical shell with liquid under longitudinal excitation". Soviet Aeronautics, vol. 19, no. 3, 1976, pp. 63-67.

[13] Obraztsova, E.I.; Shklyarchuk, F.I., "Nonlinear parametric oscillations of a cylindrical tank with a fluid". Soviet Mechanics of Solids, vol. 14, no. 4, 1979, pp. 115-126.

[14] Ramachandran, J., "Non-linear vibrations of cylindrical shells of varying thickness in an incompressible fluid". J. of Sound and Vibration, vol. 64, no. 1, 1979, pp. 97-106.

[15] Hu, W.C.L., "Free vibration of conical shells". NASA TN D-2666, (1965).

[16] Sanders, J.L., "An improved first approximation theory for thin shells". NASA-TR-R24, 1959.

[17] Love, A.E.H., "A treatise on the mathematical theory of elasticity". Dover, New-York, 1944.

[18] Singh, P.N.; Sundarajan, V.; Das, Y.C., "Large amplitude vibration of some moderately thick structural elements". J. of Sound and Vibration, vol. 36, no. 3, 1974, pp. 375-387.

[19] Anderson, J.D. jr., "Modern compressible flow with historical perspective". McGraw-Hill Series in Mechanical Engineering, 1982.

[20] Huebner, K.H., "The finite element method for engineers". A Wiley-Interscience publication, 1982.

[21] Meirovitch, L., "Analytical methods in vibrations". Macmillan Series in Applied Mechanics, 1967.

[22] Wilkinson, J.H., "The algebraic eigenvalue problem". Clarendon Press-Oxford, 1965.

[23] Ambartsumyan, S.A., "Theory of anisotropic shells". NASA TT F-118, 1961.

[24] Lakis, A.A.; Paidoussis, M.P., "Dynamic analysis of axially non-uniform thin cylindrical shells". Journal of Mechanical Science, vol. 14, no. 1, pp. 49-71, 1972.

[25] Lakis, A.A.; Paidoussis, M.P., "Shell natural frequencies of the pickering steam generators". Atomic Energy of Canada Ltd., AECL Report No. 4362, 1973.

[26] Lakis, A.A.; Paidoussis, M.P., "Free vibration of cylindrical shells partially filled with liquid". Journal of Sound and Vibration, vol. 19, pp. 1-15, 1971.

[27] Lakis, A.A.; Paidoussis, M.P., "Prediction of the response of a cylindrical shell to arbitrary or boundary-layer-induced random pressure field". Journal of Sound and Vibration, vol 25, pp. 1-27, 1972.

[28] Lakis, A.A., "Theoritical model of cylindrical structures containing turbulent flowing fluids". 2nd Int. symposium on finite element methods in flow problems, Santa Margherita Ligure (Italy), June 1976.

[29] Lakis, A.A.; Sami, S.M.; Rousselet, J., "Turbulent two phase flow loop facility for predicting wall-pressure fluctuations and shell response". 24th Int. Instrumentation Symposium Albuquerque (New-Mexico), May 1978.

[30] Sinno, M., "Vibrations naturelles des coques cylindriques partiellement remplies de liquide, axisymétriques et en comportement de poutre". Mémoire de M.Sc.A. Ecole Polytechnique de Montréal, Département de génie mécanique, Juin 1980.

[31] Toledano, A., "Analyse non-linéaire des coques cylindriques minces". Mémoire de M.Sc.A. Ecole Polytechnique de Montréal, Département de génie mécanique, Août 1982.

[32] Ouriche, H., "Analyse dynamique des coques coniques anisotropes". Mémoire de M.Sc.A. Ecole Polytechnique de Montréal, Département de génie mécanique, Avril 1984.

[33] Flugge, W., "Stresses in shells". 1960, (Springer-Verlag, Berlin).

APPENDIX A-1

SANDERS' THIN SHELL THEORY

a) General equations of equilibrium

In final format, here are the five differential equations of motion given by Sanders [16]:

$$\frac{\partial (A_2 N_{11})}{\partial \varepsilon_1} + \frac{\partial (A_1 \bar{N}_{12})}{\partial \varepsilon_2} + \frac{\bar{N}_{12} \partial A_1}{\partial \varepsilon_2} - \frac{N_{22} \partial A_2}{\partial \varepsilon_1} + \frac{A_1 A_2}{R_1} Q_1 +$$

$$\frac{A_1}{2} \frac{\partial}{\partial \varepsilon_2} \left[\left(\frac{1}{R_1} - \frac{1}{R_2} \right) \bar{M}_{12} \right] + A_1 A_2 p_1 = 0 \qquad (a1)$$

$$\frac{\partial (A_1 N_{22})}{\partial \varepsilon_2} + \frac{\partial (A_2 \bar{N}_{12})}{\partial \varepsilon_1} + \frac{\bar{N}_{12} \partial A_2}{\partial \varepsilon_1} - \frac{N_{11} \partial A_1}{\partial \varepsilon_2} + \frac{A_1 A_2}{R_2} Q_2 +$$

$$\frac{A_2}{2} \frac{\partial}{\partial \varepsilon_1} \left[\left(\frac{1}{R_1} - \frac{1}{R_2} \right) \bar{M}_{12} \right] + A_1 A_2 p_2 = 0 \qquad (a2)$$

$$\frac{\partial (A_2 Q_1)}{\partial \varepsilon_1} + \frac{\partial (A_1 Q_2)}{\partial \varepsilon_2} - A_1 A_2 \left(\frac{N_{11}}{R_1} + \frac{N_{22}}{R_2} \right) + A_1 A_2 p_n = 0 \qquad (a3)$$

$$\frac{\partial (A_2 M_{11})}{\partial \varepsilon_1} + \frac{\partial (A_1 \bar{M}_{12})}{\partial \varepsilon_2} + \bar{M}_{12} \frac{\partial A_1}{\partial \varepsilon_2} - M_{22} \frac{\partial A_2}{\partial \varepsilon_1} - A_1 A_2 Q_1 = 0 \qquad (a4)$$

$$\frac{\partial (A_1 M_{22})}{\partial \varepsilon_2} + \frac{\partial (A_1 \bar{M}_{12})}{\partial \varepsilon_1} + \bar{M}_{12} \frac{\partial A_2}{\partial \varepsilon_1} - M_{11} \frac{\partial A_1}{\partial \varepsilon_2} - A_1 A_2 Q_2 = 0 \qquad (a5)$$

with $\bar{N}_{12} = 1/2 \, (N_{12} + N_{21})$

$\bar{M}_{12} = 1/2 \, (M_{12} + M_{21})$

Figure 1 contains an illustration of these components by unit length of membrane and shear forces and the moment, with respect to the surface of reference.

b) Deformation vector

$$\varepsilon_{11} = \frac{1}{A_1}\frac{\partial u_1}{\partial E_1} + \frac{u_2}{A_1 A_2}\frac{\partial A_1}{\partial E_2} + \frac{w}{R_1}$$

$$\varepsilon_{22} = \frac{1}{A_2}\frac{\partial u_2}{\partial E_2} + \frac{u_1}{A_1 A_2}\frac{\partial A_2}{\partial E_1} + \frac{w}{R_2}$$

$$\bar{\varepsilon}_{12} = \frac{1}{2}\left[\frac{1}{A_1}\frac{\partial u_2}{\partial E_1} + \frac{1}{A_2}\frac{\partial u_1}{\partial E_2} - \frac{u_1}{A_1 A_2}\frac{\partial A_1}{\partial E_2} - \frac{u_2}{A_1 A_2}\frac{\partial A_2}{\partial E_1}\right]$$

$$\kappa_{11} = \frac{1}{A_1 A_2}\left[A_2\frac{\partial \phi_1}{\partial E_1} + \phi_2\frac{\partial A_1}{\partial E_2}\right]$$

$$\kappa_{22} = \frac{1}{A_1 A_2}\left[A_1\frac{\partial \phi_2}{\partial E_2} + \phi_1\frac{\partial A_2}{\partial E_1}\right]$$

$$\bar{\kappa}_{12} = \frac{1}{2}\left[\frac{1}{A_1}\frac{\partial \phi_2}{\partial E_1} + \frac{1}{A_2}\frac{\partial \phi_1}{\partial E_2} - \frac{1}{A_1 A_2}\left(\phi_2\frac{\partial A_2}{\partial E_1} + \phi_1\frac{\partial A_1}{\partial E_2}\right)\right.$$

$$\left. + \phi\left(\frac{1}{R_2} - \frac{1}{R_1}\right)\right]$$

with $$\phi_1 = \frac{u_1}{R_1} - \frac{1}{A_1}\frac{\partial w}{\partial E_1}$$

$$\phi_2 = \frac{u_2}{R_2} - \frac{1}{A_2}\frac{\partial w}{\partial E_2}$$

$$\phi = \frac{1}{2A_1A_2}\left[\frac{\partial(A_2u_2)}{\partial\xi_1} - \frac{\partial(A_1u_1)}{\partial\xi_2}\right]$$

c) Boundary conditions

The boundary conditions are given by:

$$N_{11} = \bar{N}_{11} \qquad \text{or} \quad u_1 = \bar{\bar{u}}_1$$

$$\bar{N}_{12} + \left(\frac{3}{R_2} - \frac{1}{R_1}\right)\frac{\bar{M}_{12}}{2} = \bar{T}_{12} \qquad \text{or} \quad u_2 = \bar{\bar{u}}_2$$

$$Q_1 + \frac{1}{A_2}\frac{\partial\bar{M}_{12}}{\partial\xi_2} = \bar{V}_1 \qquad \text{or} \quad w = \bar{\bar{w}}$$

$$M_{11} = \bar{M}_{11} \qquad \text{or} \quad \phi_1 = \bar{\bar{\phi}}_1$$

for a boundary with constant ξ_1, the double-barred terms correspond to the boundary values. For the constant ξ_2 boundary, subscripts 1 and 2 are simply interchanged.

d) Parameters for a cylindrical shell of revolution

$\xi_1 = x$	$A_1 = 1$	$R_1 = \infty$	$u_1 = U$
$\xi_2 = \theta$	$A_2 = R$	$R_2 = R$	$u_2 = V$
			$w = W$

Substituting these parameters into the five equilibrium equations (A-1, .1 to .5), we get:

$$\frac{\partial N_{xx}}{\partial x} + \frac{1}{R}\frac{\partial \bar{N}_{x\theta}}{\partial \theta} - \frac{1}{2R^2}\frac{\partial \bar{M}_{x\theta}}{\partial \theta} + P_x = 0 \qquad \text{(d1)}$$

$$\frac{1}{R}\frac{\partial N_{\theta\theta}}{\partial \theta} + \frac{\partial \bar{N}_{x\theta}}{\partial x} + \frac{1}{2R}\frac{\partial \bar{M}_{x\theta}}{\partial x} + \frac{Q_\theta}{R} + P_\theta = 0 \qquad \text{(d2)}$$

$$\frac{\partial Q_x}{\partial x} + \frac{1}{R}\frac{\partial Q_\theta}{\partial \theta} - \frac{N_{\theta\theta}}{R} + P_n = 0 \qquad \text{(d3)}$$

$$\frac{\partial M_{xx}}{\partial x} + \frac{1}{R}\frac{\partial \bar{M}_{x\theta}}{\partial \theta} - Q_x = 0 \qquad \text{(d4)}$$

$$\frac{1}{R}\frac{\partial M_{\theta\theta}}{\partial \theta} + \frac{\partial \bar{M}_{x\theta}}{\partial x} - Q_\theta = 0 \qquad \text{(d5)}$$

Elimination of shear forces Q_x and Q_θ by means of equations (d4, d5) reduces the number of equations of motion from 5 down to 3. In the absence of external loads, these equations become:

$$\frac{\partial N_{xx}}{\partial x} + \frac{1}{R}\frac{\partial \bar{N}_{x\theta}}{\partial \theta} - \frac{1}{2R^2}\frac{\partial \bar{M}_{x\theta}}{\partial \theta} = 0 \qquad \text{(d7)}$$

$$\frac{1}{R}\frac{\partial N_{\theta\theta}}{\partial \theta} + \frac{\partial \bar{N}_{x\theta}}{\partial x} + \frac{3}{2R}\frac{\partial \bar{M}_{x\theta}}{\partial x} + \frac{1}{R^2}\frac{\partial M_{\theta\theta}}{\partial \theta} = 0 \qquad \text{(d8)}$$

$$\frac{\partial^2 M_{xx}}{\partial x^2} + \frac{2}{R}\frac{\partial^2 \bar{M}_{x\theta}}{\partial x \partial \theta} + \frac{1}{R^2}\frac{\partial^2 M_{\theta\theta}}{\partial \theta^2} - \frac{N_{\theta\theta}}{R} = 0 \qquad \text{(d9)}$$

Substituting these parameters into the deformation vector we get:

$$\{\varepsilon\} = \begin{Bmatrix} \dfrac{\partial u}{\partial x} \\ \dfrac{1}{R}\left(\dfrac{\partial v}{\partial \theta} + w\right) \\ \dfrac{\partial v}{\partial x} + \dfrac{1}{R}\dfrac{\partial u}{\partial \theta} \\ -\dfrac{\partial^2 w}{\partial x^2} \\ \dfrac{1}{R^2}\left(\dfrac{\partial^2 w}{\partial \theta^2} - \dfrac{\partial v}{\partial \theta}\right) \\ -\dfrac{2}{R}\dfrac{\partial^2 w}{\partial x \partial \theta} + \dfrac{3}{2R}\dfrac{\partial v}{\partial x} - \dfrac{1}{2R^2}\dfrac{\partial u}{\partial \theta} \end{Bmatrix} \quad \text{(d10 to d15)}$$

The reference surface geometry of the shell studied together with the coordinates used are illustrated in Figure 3.

APPENDIX A-2

EQUATIONS OF MOTION

This appendix contains the equations of motion for a thin cylindrical anisotropic shell which were referenced in the different chapters of this paper.

$$L_1(U,V,W,P_{ij}) = P_{11}\frac{\partial^2 U}{\partial x^2} + \frac{P_{12}}{R}\left(\frac{\partial^2 V}{\partial x\partial\theta} + \frac{\partial W}{\partial x}\right) - P_{14}\frac{\partial^3 W}{\partial x^3} +$$

$$\frac{P_{15}}{R^2}\left(-\frac{\partial^3 W}{\partial x\partial\theta^2} + \frac{\partial^2 V}{\partial x\partial\theta}\right) + \left(\frac{P_{33}}{R} - \frac{P_{63}}{2R^2}\right)\left(\frac{\partial^2 V}{\partial x\partial\theta} - \frac{1}{R}\frac{\partial^2 U}{\partial\theta^2}\right) +$$

$$\left(\frac{P_{36}}{R^2} - \frac{P_{66}}{2R^3}\right)\left(-\frac{2\partial^3 W}{\partial x\partial\theta^2} + \frac{3}{2}\frac{\partial^2 V}{\partial x\partial\theta} - \frac{1}{2R}\frac{\partial^2 U}{\partial\theta^2}\right) \qquad (1)$$

$$L_2(U,V,W,P_{ij}) = \left(\frac{P_{21}}{R} + \frac{P_{51}}{R^2}\right)\frac{\partial^2 U}{\partial x\partial\theta} + \frac{1}{R}\left(\frac{P_{22}}{R} + \frac{P_{52}}{R^2}\right)$$

$$\left(\frac{\partial^2 V}{\partial\theta^2} + \frac{\partial W}{\partial\theta}\right) - \left(\frac{P_{24}}{R} + \frac{P_{54}}{R^2}\right)\left(\frac{\partial^3 W}{\partial x^2\partial\theta}\right) + \frac{1}{R^2}\left(\frac{P_{25}}{R} + \frac{P_{55}}{R^2}\right)$$

$$\left(-\frac{\partial^3 W}{\partial\theta^3} + \frac{\partial^2 V}{\partial\theta^2}\right) + \left(P_{33} + \frac{3P_{63}}{2R}\right)\left(\frac{\partial^2 V}{\partial x^2} + \frac{\partial^2 U}{R\partial x\partial\theta}\right) +$$

$$\frac{1}{R}\left(P_{36} + \frac{3P_{66}}{2R}\right)\left(-2\frac{\partial^3 W}{\partial x^2\partial\theta} + \frac{3}{2}\frac{\partial^2 V}{\partial x^2} - \frac{\partial^2 U}{2R\partial x\partial\theta}\right) \qquad (2)$$

$$L_3(U,V,W,P_{ij}) = P_{41}\frac{\partial^3 U}{\partial x^3} + \frac{P_{42}}{R}\left(\frac{\partial^3 V}{\partial x^2\partial\theta} + \frac{\partial^2 W}{\partial x^2}\right) - P_{44}\frac{\partial^4 W}{\partial x^4}$$

$$+ \frac{P_{45}}{R^2}\left(-\frac{\partial^4 W}{\partial x^2\partial\theta^2} + \frac{\partial^3 V}{\partial x^2\partial\theta}\right) + \frac{2P_{63}}{R}\left(\frac{\partial^3 U}{R\partial x\partial\theta} + \frac{\partial^3 V}{\partial x^2\partial\theta}\right) + \frac{2P_{66}}{R^2}$$

$$\left(-2\frac{\partial^4 W}{\partial x^2\partial\theta^2} + \frac{3}{2}\frac{\partial^3 V}{\partial x^2\partial\theta} - \frac{\partial^3 U}{2R\partial x\partial\theta^2}\right) + \frac{P_{51}}{R^2}\frac{\partial^3 U}{\partial x\partial\theta^2} + \frac{P_{52}}{R^3}\left(\frac{\partial^3 V}{\partial\theta^3} +\right.$$

$$\left.\frac{\partial^2 W}{\partial\theta^2}\right) + \frac{P_{55}}{R^4}\left(-\frac{\partial^4 W}{\partial\theta^4} + \frac{\partial^3 V}{\partial\theta^3}\right) - \frac{P_{21}}{R}\frac{\partial U}{\partial x} - \frac{P_{54}}{R^2}\frac{\partial^4 W}{\partial x^2\partial\theta^2} - \frac{P_{22}}{R^2}\left(\frac{\partial V}{\partial\theta}\right.$$

$$\left.+ W\right) + \frac{P_{24}}{R}\frac{\partial^2 W}{\partial x^2} - \frac{P_{25}}{R^3}\left(-\frac{\partial^2 W}{\partial\theta^2} + \frac{\partial V}{\partial\theta}\right) \qquad (3)$$

APPENDIX A-3

Matrix of Elasticity

The elasticity matrix depends solely on the mechanical properties of the material making up the shell. We shall limit our analysis to the particular anisotropic case of a shell of revolution commonly called orthotropy, where the mechanical characteristics are invariant in rotation around a fixed axis.

For anisotropic material [23], [P] is generally written in the form:

$$[P] = \begin{bmatrix} P_{11} & P_{12} & 0 & P_{14} & P_{15} & 0 \\ P_{21} & P_{22} & 0 & P_{24} & P_{25} & 0 \\ 0 & 0 & P_{33} & 0 & 0 & P_{36} \\ P_{41} & P_{42} & 0 & P_{44} & P_{45} & 0 \\ P_{51} & P_{52} & 0 & P_{54} & P_{55} & 0 \\ 0 & 0 & P_{36} & 0 & 0 & P_{66} \end{bmatrix}$$

For a shell made up of a number of symmetric layers of iso- or orthotropic material arranged as in Figure 4, elements P_{ij} of [P] are expressed as follows:

- for number of layers 2v:

$$P_{ij} = 2 \sum_{s=1}^{v} B_{ij}^{s} (\delta_s - \delta_{s+1})$$

with i = 1 to 3 and j = 1 to 6

$$P_{ij} = \frac{2}{3} \sum_{s=1}^{v} B_{i-3,j-3}^{s} (\delta_s^3 - \delta_{s+1}^3)$$

with i = 4 to 6 and j = 4 to 6

- for number of layers 2v + 1:

$$p_{ij} = 2 \left[B_{ij}^{v+1} \delta_{v+1} + \sum_{s=1}^{v} B_{ij}^{s} (\delta_s - \delta_{s+1}) \right]$$

with i = 1 to 3 and j = 1 to 6

$$p_{ij} = \frac{2}{3} \left[B_{i-3,j-3}^{v+1} \delta_{v+1}^{3} + \sum_{s=1}^{v} B_{i-3,j-3}^{s} (\delta_s^3 - \delta_{s+1}^3) \right]$$

with i = 4 to 6 and j = 4 to 6

where: $B_{11}^{s} = \dfrac{E_1^s}{(1 - \nu_1^s \nu_2^s)}$

$$B_{12}^{s} = B_{21}^{s} = \frac{\nu_2 E_1}{(1 - \nu_1^s \nu_2^s)}$$

$$B_{22}^{s} = \frac{E_2^s}{(1 - \nu_1^s \nu_2^s)}$$

$$B_{33}^{s} = 0.5\, G_{12}^{s}$$

$$B_{ij}^{s} = 0 \qquad \text{elsewhere}$$

- δ_s : coordinate of the s^{th} layer with the average surface as reference.

- (E_1^s, ν_1^s), (E_2^s, ν_2^s): Young's modulus and Poisson's ratio, respectively, with respect to axes x and θ.

- G_{12}^s : shear elastic modulus

For an isotropic cylindrical shell made up of a layer of constant thickness t, we have:

$$[P] = \begin{bmatrix} D & \nu D & 0 & 0 & 0 & 0 \\ \nu D & D & 0 & 0 & 0 & 0 \\ 0 & 0 & \frac{(1-\nu)D}{2} & 0 & 0 & 0 \\ 0 & 0 & 0 & K & \nu K & 0 \\ 0 & 0 & 0 & \nu K & K & 0 \\ 0 & 0 & 0 & 0 & 0 & \frac{(1-\nu)K}{2} \end{bmatrix}$$

with D : membrane stiffness

K : bending stiffness

$$D = \frac{E\,t}{1 - \nu^2}$$

$$K = \frac{E\,t^3}{12\,(1 - \nu^2)}$$

APPENDIX A-4

Nodal Interpolation Functions

The shell of revolution is a continuous deformable medium with an infinite number of degrees of freedom. Its state of equilibrium is governed by the equations in Appendix A-2. The original shell is partitioned into a number of finite elements having, therefore, a finite number of degrees of freedom. By carefully selecting the displacement functions we convert our differential partial equilibrium equations into a system of linear algebraic equations.

As displacements are periodic in the circumferential direction, we assume that the displacement functions can be expressed by expansion into a Fourier series.

$$\{u(x,\theta),w(x,\theta),v(x,\theta)\}^t=\sum_{n=1}^{\infty}[T(n,\theta)]\{u_n(x),w_n(x),v_n(x)\}^t \qquad (a)$$

where n: circumferential mode number
$[T]$: square diagonal matrix given in Appendix A-5.

Let us set:

$$u(x) = A\, e^{\lambda x/R}$$

$$v(x) = B\, e^{\lambda x/R} \qquad (b)$$

$$w(x) = C\, e^{\lambda x/R}$$

Inserting the expressions for displacement functions given in (a) and (b) into the (App. A-2) system of equations, we obtain a system of algebraic equations of the form:

$$[H]\ \{A,B,C\}^t = \{0\} \qquad (c)$$

So that the solution is non-trivial, the [H] determinant must be zero. This gives us the characteristic equation:

$$\det([H]) = h_8\lambda^8 - h_6\lambda^6 + h_4\lambda^4 - h_2\lambda^2 + h_0 = 0 \qquad (d)$$

The h_i expression in this fourth-degree polynomial in λ^2 is given in Appendix A-5.

Each λ_i root gives a displacement $\{u_n(x), w_n(x), v_n(x)\}_i^t$.

The complete solution is obtained by linear combination of these eight displacements. This therefore gives us:

$$u_n(x) = \sum_{p=1}^{8} A_p e^{\lambda_p x/R}$$

$$v_n(x) = \sum_{p=1}^{8} B_p e^{\lambda_p x/R} \qquad (e)$$

$$w_n(x) = \sum_{p=1}^{8} C_p e^{\lambda_p x/R}$$

Constants A_p, B_p and C_p are interconnected by (c). A_p and B_p are usually expressed in terms of C_p.

Let us set:

$$A_p = \alpha_p C_p \quad \text{and} \quad B_p = \beta_p C_p \qquad \text{with } p = 1,\ldots 8 \qquad (f)$$

The α_p and β_p expressions are obtained from the following relations:

$$\begin{bmatrix} H_{11} & H_{12} \\ H_{21} & H_{22} \end{bmatrix} \begin{Bmatrix} \alpha_p \\ \beta_p \end{Bmatrix} = \begin{Bmatrix} -H_{13} \\ -H_{23} \end{Bmatrix} \qquad (g)$$

where the H_{kl} coefficients are given in Appendix A-5.

Equation (a) is then expressed in terms of the eight C_p constants by expressions (e) and (f). We then obtain:

$$\{u(x,\theta),w(x,\theta),v(x,\theta)\}^t = [T]\,[R]\,\{C\} \qquad (h)$$

where: [R] 3 X 8 matrix given in Appendix A-5
{C} column vector for the eight C_p constants

Setting [R] = [L] [X], the (h) equation becomes:

$$\{u(x,\theta),w(x,\theta),v(x,\theta)\}^t = [T]\,[L]\,[X]\,\{C\} \qquad (i)$$

For particular circumferential mode n, displacement of any physical point m(x,θ) may be expressed in terms of degrees of freedom $\{\delta_i\}$ and $\{\delta_j\}$ of nodes i and j on the finite element on which the point is located.

The nodal displacements at element boundary i (x = 0) and j (x = 1) will be:

$$\begin{Bmatrix}\delta i\\ \delta j\end{Bmatrix} = \{u_{ni}, w_{ni}, \frac{\partial w_{ni}}{\partial x}_i, v_{ni}, u_{nj}, w_{nj}, \frac{\partial w_{nj}}{\partial x}_j, v_{nj}\} = [A]\{C\} \qquad (j)$$

where the [A] terms, given in Appendix A-5, are obtained by successive applications of the boundary conditions to [R].

Multiplying (j) by $[A^{-1}]$, we obtain:

$$\{C\} = [A^{-1}] \begin{Bmatrix}\delta_i\\ \delta_j\end{Bmatrix} \qquad (k)$$

The (j) relation is then written:

$$\{u,w,v\}^t = [T]\,[L]\,[X]\,[A^{-1}] \begin{Bmatrix}\delta_i\\ \delta_j\end{Bmatrix} \qquad (l)$$

that is: $\{u,w,v\}^t = [N] \begin{Bmatrix} \delta_i \\ \delta_j \end{Bmatrix}$ (m)

with $[N] = [T]\,[L]\,[X]\,[A^{-1}]$

where [N] : 3 X 8 matrix
Exact nodal interpolation function defining displacement of point M.

The resultant displacement is therefore:

$$\{u,w,v\}^t = \sum_{n=0}^{\infty} [N] \begin{Bmatrix} \delta_i \\ \delta_j \end{Bmatrix} \quad \text{(n)}$$

APPENDIX A-5

MATRICES

This appendix contains the matrices which were referenced in the course of the various analytical developments.

The matrices are classified as follows:

[H]	(table 1)
[A]	(table 2)
[T] , [L] , [X]	(table 3)
[J]	(table 4)

The eight roots of the characteristic equation (Appendix A-6) are represented by λ_p (p=1, ..., 8). The values for α_p and β_p are defined by equations (A-4,g).

The l and R terms are the length and radius, respectively, of each finite element.

TABLE 1

MATRIX [H]
(3,3)

$$[H]\begin{Bmatrix} A \\ B \\ C \end{Bmatrix} = \{0\} \qquad ;[H]=\begin{bmatrix} H_{11} & H_{12} & H_{13} \\ H_{21} & H_{22} & H_{23} \\ H_{31} & H_{32} & H_{33} \end{bmatrix}$$

Here, we will only be giving the coefficients appearing in equation (A-4,g).

$$H_{11} = n^2 h_1 - \lambda^2 p_{11}$$

$$H_{12} = -n\lambda h_3$$

$$H_{21} = H_{12}$$

$$H_{22} = -n^2 h_7 + \lambda^2 h_9$$

$$H_{13} = -\lambda(n^2 h_5 + p_{12}) + \frac{\lambda^3 p_{14}}{R}$$

$$H_{23} = -n(1 + n^2)\frac{p_{25}}{R} - np_{22} - n^3\frac{p_{55}}{R^2} + n\lambda^2 h_{11}$$

with $$h_1 = p_{33} - \frac{p_{36}}{R} + \frac{p_{66}}{4R^2}$$

$$h_3 = p_{12} + p_{33} + \frac{(p_{15} + p_{36})}{R} - \frac{3p_{66}}{4R^2}$$

$$h_5 = \frac{\left(p_{15} + 2p_{36} - \frac{p_{66}}{R} \right)}{R}$$

$$h_7 = p_{22} + \frac{p_{55}}{R^2} + \frac{2p_{25}}{R}$$

$$h_9 = p_{33} + \frac{3p_{36}}{R} + \frac{9p_{66}}{4R^2}$$

$$h_{11} = \frac{(2p_{36} + p_{24} + \frac{3p_{66}}{R} + \frac{p_{54}}{R})}{R}$$

TABLE 2

MATRIX [A]
(8,8)

$$\begin{Bmatrix} \delta_i \\ \delta_j \end{Bmatrix} = \underset{(8,8)}{[A]} \quad \underset{(8,1)}{\{C\}}$$

with $\{C\} = \{C_1, C_2, \ldots, C_8\}^t$

$$\begin{Bmatrix} \delta_i \\ \delta_j \end{Bmatrix} = \{u_i \;\; w_i \;\; \frac{\partial w}{\partial x}_i \;\; v_i \;\; u_j \;\; w_j \;\; \frac{\partial w}{\partial x}_j \;\; v_j\}^t$$

$A(1,q) = \alpha_q$

$A(2,q) = 1$

$A(3,q) = \frac{\lambda_q}{R}$

$A(4,q) = \beta_q$

$A(5,q) = A(1,q)\; a_q$

$A(6,q) = A(2,q)\; a_q$

$A(7,q) = A(3,q)\; a_q$

$A(8,q) = A(4,q)\; a_q$

$$a_q = e^{\frac{\lambda_q \; 1}{R}} \qquad \text{and } q = 1, \ldots, 8$$

TABLE 3

MATRICES [T] , [L] , [X]
(3,3) (3,8) (8,8)

$$\begin{Bmatrix} U(x,\theta) \\ W(x,\theta) \\ V(x,\theta) \end{Bmatrix} = \underset{(3,3)}{[T]} \quad \underset{(3,8)}{[L]} \quad \underset{(8,8)}{[X]} \quad \underset{(8,1)}{\{C\}}$$

with $\{C\} = \{C_1, C_2, \ldots, C_8\}^t$

$$[T] = \begin{bmatrix} \cos n\theta & 0 & 0 \\ 0 & \cos n\theta & 0 \\ 0 & 0 & \sin n\theta \end{bmatrix}$$

$L(1,q) = \alpha_q$

$L(2,q) = 1$ $\qquad q = 1, \ldots, 8$

$L(3,q) = \beta_q$

$X(p,q) = e^{\frac{\lambda_q x}{R}}$ $\qquad$ if $p = q$

$X(p,q) = 0$ $\qquad$ if $p \neq q$ $\qquad p,q = 1, \ldots, 8$

TABLE 4

MATRIX [J]
(6,8)

$$\{\varepsilon\} = \underset{(6,6)}{\begin{bmatrix} [T] & [O] \\ [O] & [T] \end{bmatrix}} \quad \underset{(6,8)}{[J]} \quad \underset{(8,8)}{[X]} \quad \underset{(8,8)}{[A^{-1}]} \quad \underset{(8,1)}{\begin{Bmatrix} \delta_i \\ \delta_j \end{Bmatrix}}$$

with $J(1,q) = \alpha_q \frac{\lambda_q}{R}$

$J(2,q) = \frac{1}{R}(n\beta_q + 1)$

$J(3,q) = \frac{1}{R}(\beta_q\lambda_q - n\alpha_q)$

$q = 1, \ldots, 8$

$J(4,q) = -(\frac{\lambda_q}{R})^2$

$J(5,q) = \frac{1}{R^2}(n^2 + \beta_q n)$

$J(6,q) = \frac{1}{R^2}(2n\lambda_q + \frac{3}{2}\beta_q\lambda_q + \frac{1}{2}n\alpha_q)$

APPENDIX A-6

CHARACTERISTIC EQUATION COEFFICIENTS

The characteristic equation (A-4,d) is:

$$h_8\lambda^8 - h_6\lambda^6 + h_4\lambda^4 - h_2\lambda^2 + h_0 = 0$$

where: $h_8 = \frac{h_9}{r^2}\,(p_{11}p_{44} - p_{14}^2)$

$$h_6 = \frac{n^2}{r^2}\,[h_9(h_1p_{44} + 2p_{11}p_{45} + 4p_{11}p_{66} - 2h_5rp_{14}) +$$

$$h_7(p_{11}p_{44} - p_{14}^2) - r^2h_{11}^2p_{11} - h_3^2p_{44} + 2rh_3h_{11}p_{14}] +$$

$$\frac{2}{r}\,h_9(p_{11}p_{24} - p_{14}p_{12})$$

$$h_4 = (\frac{n^4}{r^2})\,[h_1h_7p_{44} + h_9p_{11}p_{55} + (2p_{45} + 4p_{66})\,(h_1h_9 +$$

$$h_7p_{11} - h_3^2) + (p_{25} + \frac{p_{55}}{r})\,.\,(2h_3p_{14} - 2h_{11}p_{11}r) +$$

$$h_{11}r^2(2h_3h_5 - h_1h_{11}) - rh_5\,(2h_7p_{14} + rh_5h_9)] +$$

$$(\frac{n^2}{r})\,.\,[2\,(p_{25} + rp_{22})\,((\frac{h_3p_{14}}{r}) - h_{11}p_{11}) -$$

$$2p_{12}(h_5h_9r + h_7p_{14} - h_3h_{11}r) - 2p_{24}\ (h_3^2 - h_1h_9 -$$

$$h_7p_{11}) + 2h_9p_{11}p_{25}] + h_9\ (p_{11}p_{22} - p_{12}^2)$$

$$h_2 = \left(\frac{n^6}{r^2}\right)\ [h_1h_7(2p_{45} + 4p_{66}) + p_{55}(h_1h_9 + h_7p_{11} - h_3^2) -$$

$$r^2h_5^2h_7 + \left(p_{25} + \frac{p_{55}}{r}\right)\ .\ (-2rh_1h_{11} + 2rh_3h_5 - p_{11}p_{25}$$

$$-\frac{p_{11}p_{55}}{r}] + \frac{n^4}{r}\ [2h_1h_7p_{24} + 2p_{25}(h_1h_9 + h_7p_{11} - h_3^2)$$

$$- 2p_{12}(rh_5h_7 - h_3p_{25} - \frac{h_3p_{55}}{r} - 2\ (p_{25} + rp_{22})\ .$$

$$(h_1h_{11} + \frac{p_{11}p_{25}}{r} + \frac{p_{11}p_{55}}{r^2} - h_3h_5)] +$$

$$n^2[p_{22}(h_1h_9 + h_7p_{11} - h_3^2) - \frac{(p_{25} + rp_{22})}{r}\ .$$

$$(\left(\frac{p_{11}p_{25}}{r} + p_{11}p_{22} - 2h_3p_{12}\right) - h_7p_{12}^2]$$

$$h_0 = n^4h_1h_7\ [p_{22} + \frac{2n^2p_{25}}{r} + \frac{n^4p_{55}}{r^2}] - n^2h_1$$

$$[\left(\frac{n^3}{r}\right)\ \left(p_{25} + \frac{p_{55}}{r}\right) + \left(\frac{n}{r}\right)\ (p_{25} + rp_{22})]^2$$

APPENDIX B-1

Equation for Non-rotational and Non-viscous Flow

Here we have:

$$\nabla^2\phi = \frac{1}{c^2}\left[\vec{\nabla}\phi \cdot (\vec{\nabla}\phi \cdot \vec{\nabla})\,\vec{\nabla}\phi + \phi_{,tt} + 2\,\vec{\nabla}\phi \cdot \vec{\nabla}\phi_{,t}\right] \qquad (a)$$

and $\vec{V} = \vec{\nabla}\phi$

In terms of its components, the velocity vector is written:

$$\vec{V} = (U_x + \phi_{,x})\,\vec{e}_x + \frac{\phi_{,\theta}}{r}\,\vec{e}_\theta + \phi_{,r}\vec{e}_r \qquad (b)$$

Substituting relation (b) into (a), we obtain:

$$\nabla^2\phi = \frac{1}{c^2}\Big\{ (U_x + \phi_{,x})^2\,\phi_{,xx} + \frac{2}{r^2}(U_x + \phi_{,x})\,\phi_{,\theta}\phi_{,x\theta}$$

$$+ 2(U_x + \phi_{,x})\,\phi_{,r}\phi_{,rx} + \frac{2}{r^2}\,\phi_{,\theta}\phi_{,r}\phi_{,r\theta} + \left(\frac{\phi_{,\theta}}{r^4}\right)^2\phi_{,\theta\theta}$$

$$- \frac{\phi_{,r}}{r^3}(\phi_{,\theta})^2 + (\phi_{,r})^2\phi_{,rr} + \phi_{,tt} +$$

$$2\left[\phi_{,xt}(U_x + \phi_{,x}) + \frac{\phi_{,\theta}}{r^2}\,\phi_{,\theta t} + \phi_{,r}\phi_{,rt}\right]\Big\} \qquad (c)$$

We extract the linear component from this last expression in order to obtain the expression given in (4.2).

APPENDIX B-2

Bernoulli Equation for Ideal Flow

This is the Euler ideal flow equation where the contribution by the external forces is considered equal to the scalar potential of the gradient.

$$\frac{\partial \vec{U}}{\partial t} + (\vec{U} \cdot \vec{\nabla})\,\vec{U} = -\frac{\vec{\nabla} p}{\rho} - \vec{\nabla}\omega \qquad \text{(a)}$$

Where $\vec{U}$: vector area for flow velocity
p : scalar pressure area
ω : scalar potential associated with external forces
ρ : fluid density

We obtain the Bernoulli equation by integrating relation (a) along a streamline allowing for the hypotheses stated in Chapter 2.

$$\frac{\partial \varphi}{\partial t} + \frac{U^2}{2} + \omega + \frac{p}{\rho} = K \qquad \text{(b)}$$

where K is an arbitrary constant.

In the absence of external forces, we revert to the usual form of the Bernoulli equation.

$$\frac{\partial \varphi}{\partial t} + \frac{U^2}{2} + \frac{p}{\rho} = 0 \qquad \text{(c)}$$

We thus obtain expression (4.6) by associating the velocity fields defined in (4.14) with $\vec{U}$ and substituting this expression into relation (c).

APPENDIX C

Model	No. 1 ; Reynolds Number: $R_N = 1.0 \times 10^6$		
Axial mode m	Eigenvalue λ_i (asymmetric case)	Eigenvalue λ_i (symmetric case)	% variance
1	0.33135×10^3	0.33139×10^3	0.012
2	0.11101×10^4	0.11099×10^4	0.018
3	0.23497×10^4	0.23480×10^4	0.072
4	0.39835×10^4	0.39739×10^4	0.241
5	0.12058×10^5	0.12002×10^5	0.464
6	0.14969×10^5	0.14668×10^5	2.011
7	0.21754×10^5	0.20016×10^5	7.990
8	0.29544×10^5	0.25143×10^5	14.90
9	0.32166×10^5	0.28751×10^5	10.62
10	0.32497×10^5	0.29926×10^5	7.912
11	0.32605×10^5	0.33276×10^5	2.058
12	0.33631×10^5	0.33282×10^5	1.037

Table 1: Validation of the proposed model for flow conditions

Model	No. 2 ; Reynolds Number: $R_N = 1.0 \times 10^6$		
Axial mode m	Eigenvalue λ_i (asymmetric case)	Eigenvalue λ_i (symmetric case)	% variance
1	0.95365×10^3	0.95422×10^3	0.060
2	0.10471×10^4	0.10470×10^4	0.010
3	0.13394×10^4	0.13391×10^4	0.022
4	0.18845×10^4	0.18841×10^4	0.021
5	0.31266×10^4	0.31263×10^4	0.010
6	0.41399×10^4	0.41382×10^4	0.041
7	0.60470×10^4	0.60411×10^4	0.098
8	0.91640×10^4	0.91412×10^4	0.249
9	0.14379×10^5	0.14277×10^5	0.709
10	0.18409×10^5	0.18175×10^5	1.270
11	0.27930×10^5	0.28033×10^5	0.369
12	0.28057×10^5	0.28099×10^5	0.150

Table 2: Validation of the proposed mode for flow conditions

Model	No. 3 ; Reynolds Number: R_N = 0.0		
Axial mode m	Eigenvalue λ_i (asymmetric case)	Eigenvalue λ_i (symmetric case)	% variance
1	0.10960×10^4	0.10958×10^4	0.018
2	0.36149×10^4	0.36032×10^4	0.324
3	0.68349×10^4	0.67494×10^4	1.251
4	0.10127×10^5	0.98589×10^4	2.647
5	0.33425×10^5	0.26910×10^5	19.49
6	0.34021×10^5	0.27880×10^5	18.05
7	0.35865×10^5	0.30030×10^5	16.27
8	0.35948×10^5	0.31801×10^5	11.54
9	0.36050×10^5	0.32021×10^5	11.18
10	0.36221×10^5	0.32259×10^5	10.94
11	0.36497×10^5	0.38303×10^5	4.950
12	0.36801×10^5	0.39870×10^5	8.340

Table 3: Validation of the proposed model for no-flow conditions

Model	No. 4 ; Reynolds Number: R_N = 0.0		
Axial mode m	Eigenvalue λ_i (asymmetric case)	Eigenvalue λ_i (symmetric case)	% variance
1	0.33156×10^2	0.33156×10^2	0.000
2	0.11102×10^3	0.11101×10^3	0.009
3	0.23498×10^3	0.23482×10^3	0.290
4	0.39836×10^3	0.39742×10^3	0.236
5	0.12058×10^4	0.12002×10^4	0.464
6	0.14969×10^4	0.14668×10^4	2.011
7	0.21755×10^4	0.20017×10^4	7.990
8	0.29544×10^4	0.25143×10^4	14.92
9	0.32153×10^4	0.28752×10^4	10.58
10	0.32496×10^4	0.29927×10^4	7.912
11	0.32547×10^4	0.32276×10^4	0.833
12	0.33990×10^4	0.33276×10^4	2.100

Table 4: Validation of the proposed model for no-flow conditions

SYNOPTIC TABLE

Model					Axial mode coupling			Axial mode uncoupling		
No.	Experimental parameters				Range of values		3rd axial mode	Range of values		3rd axial mode
	n	$\frac{L}{R}$	Young's modulus	Reynolds number R_N	$\frac{\omega_{NL}}{\omega_L}$	$\frac{A}{t}$		$\frac{\omega_{NL}}{\omega_L}$	$\frac{A}{t}$	
1	3	6	E steel	$0. \times 10^0$	0.875 @ 1.000	10^8 @ 10^{14}	10-12-9	0.800 @ 1.000	10^9 @ 10^{18}	9-7-10
				$1. \times 10^6$	0.990 @ 1.000	10^{13} @ 10^{23}	1-3-2	0.935 @ 1.000	10^{14} @ 10^{27}	1-3-7
				$2. \times 10^6$	0.997 @ 1.000	10^{13} @ 10^{23}	1-3-2	0.950 @ 1.000	10^{13} @ 10^{26}	1-3-7
2	6	6	E steel	$0. \times 10^0$	0.935 @ 1.000	10^8 @ 10^{14}	11-10-12	0.800 @ 1.000	10^9 @ 10^{17}	12-10-11
				$1. \times 10^6$	0.992 @ 1.000	10^{17} @ 10^{22}	1-3-7	0.925 @ 1.000	10^{17} @ 10^{26}	1-3-7
3	3	3	E steel	$0. \times 10^0$	0.900 @ 1.000	10^{12} @ 10^{17}	12-9-7	0.800 @ 1.000	10^{12} @ 10^{23}	12-10-7
				$1. \times 10^6$	0.990 @ 1.000	10^{23} @ 10^{31}	2-9-11	0.910 @ 1.000	10^{24} @ 10^{31}	2-11-10
4	3	6	$\frac{E_{steel}}{100}$	$0. \times 10^0$	0.900 @ 1.000	10^8 @ 10^{14}	10-12-9	0.800 @ 1.000	10^9 @ 10^{18}	9-7-10
				$1. \times 10^6$	0.998 @ 1.000	10^8 @ 10^{18}	1-3-2	0.900 @ 1.000	10^9 @ 10^{23}	1-3-2

Table 5: Influence of different experimental parameters on their relative contribution to variations in the frequency ratio

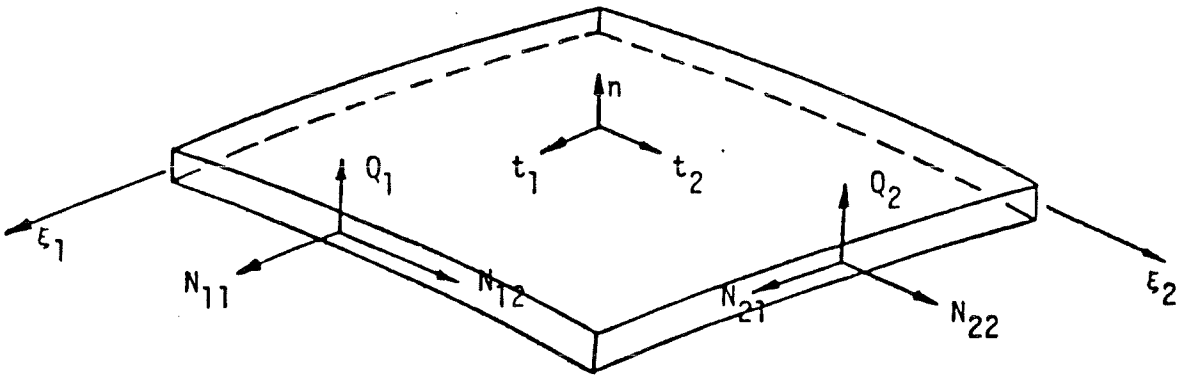

Direction of resultant constraints

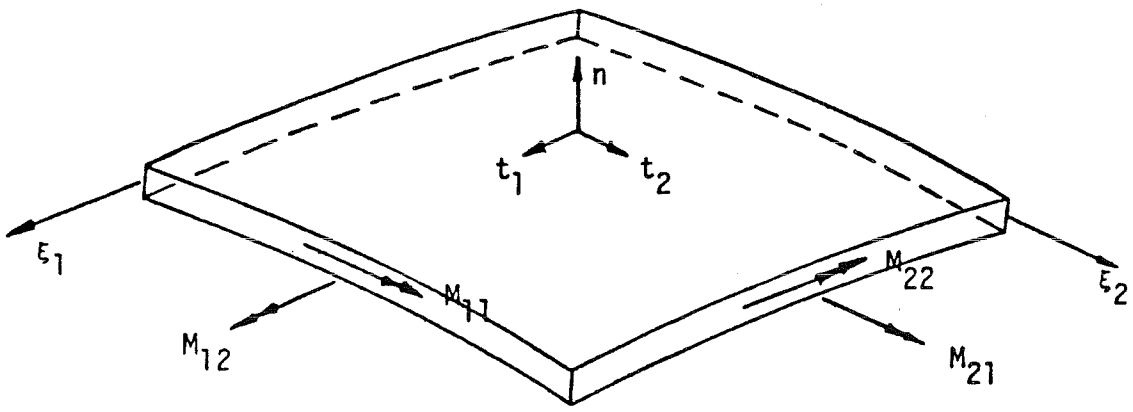

Direction of resultant moments

FIGURE 1: Differential element for a thin shell

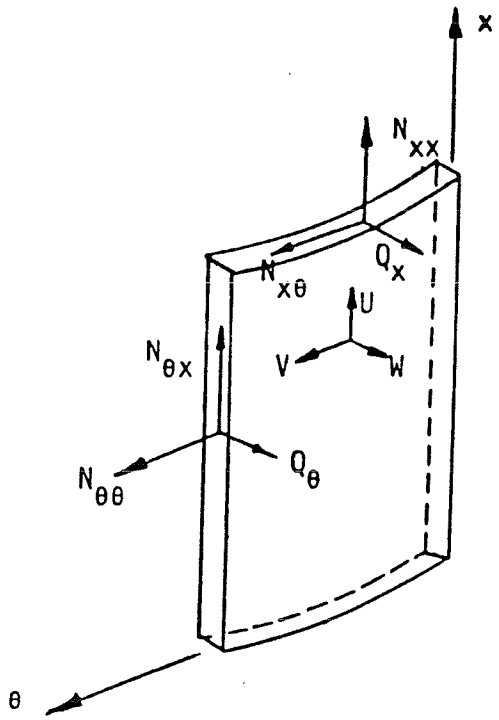

(a) Resultant constraints and displacements

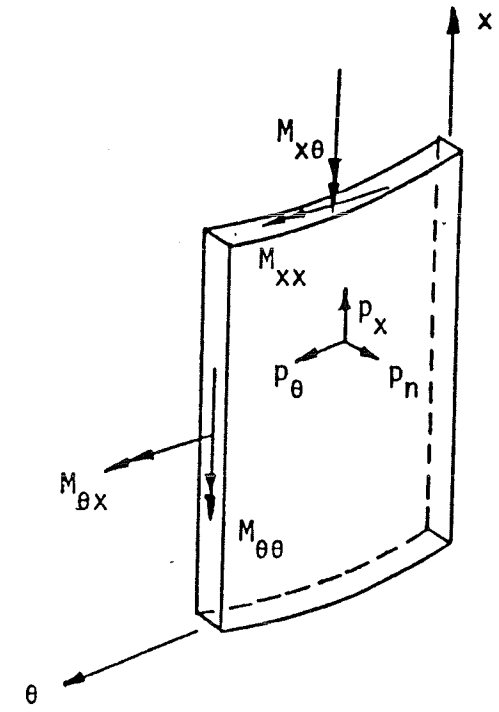

(b) Resultant couples and external loads

FIGURE 2: Differential element for a cylindrical shell

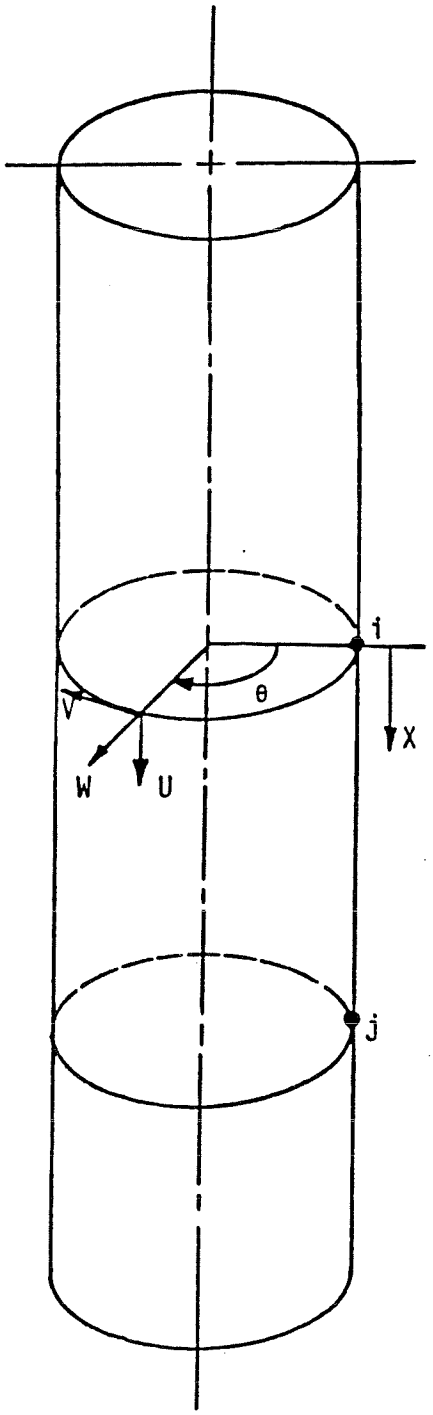

FIGURE 3: Reference surface geometry for a cylindrical shell

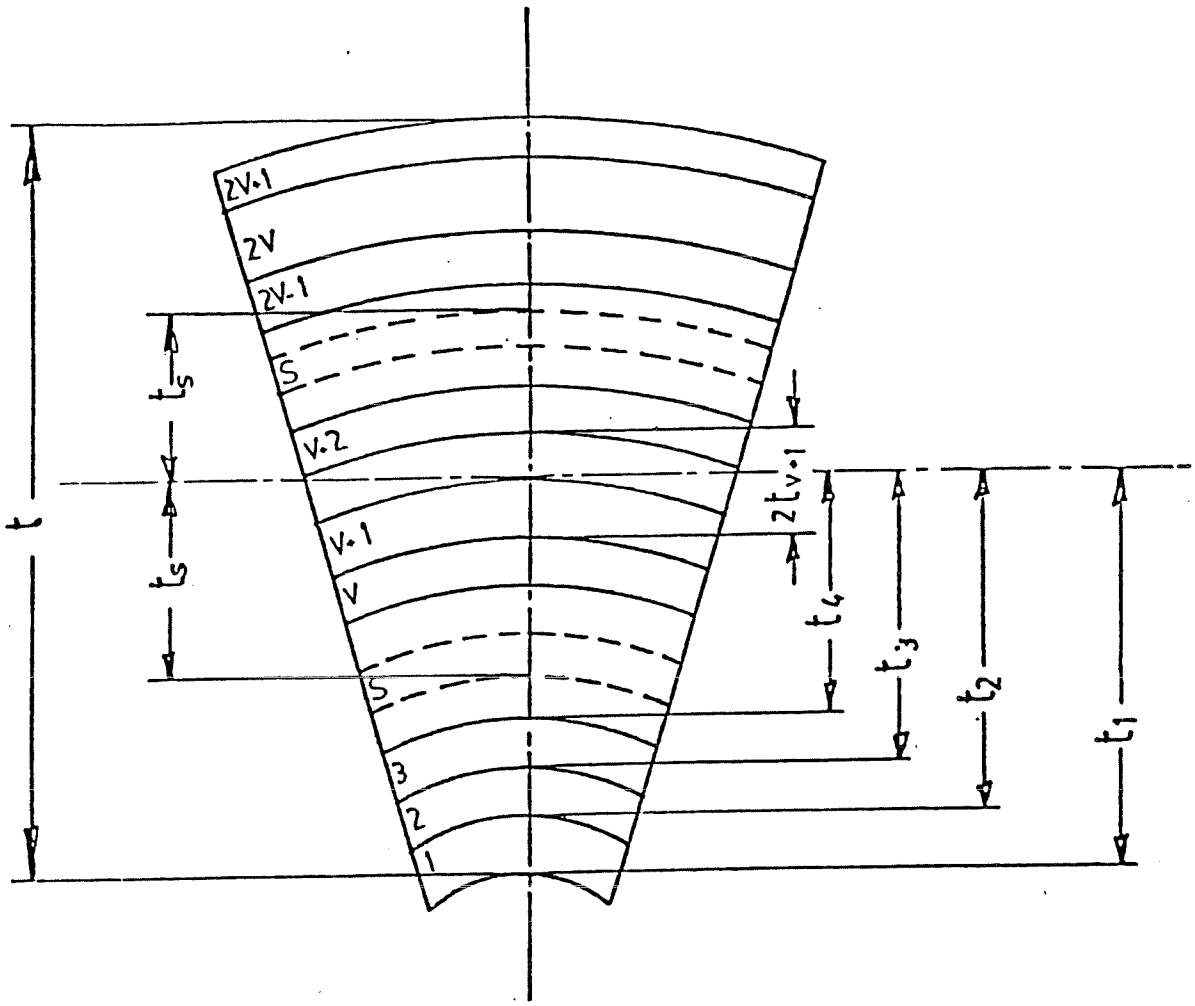

FIGURE 4: Shell made up of an odd number of anisotropic layers

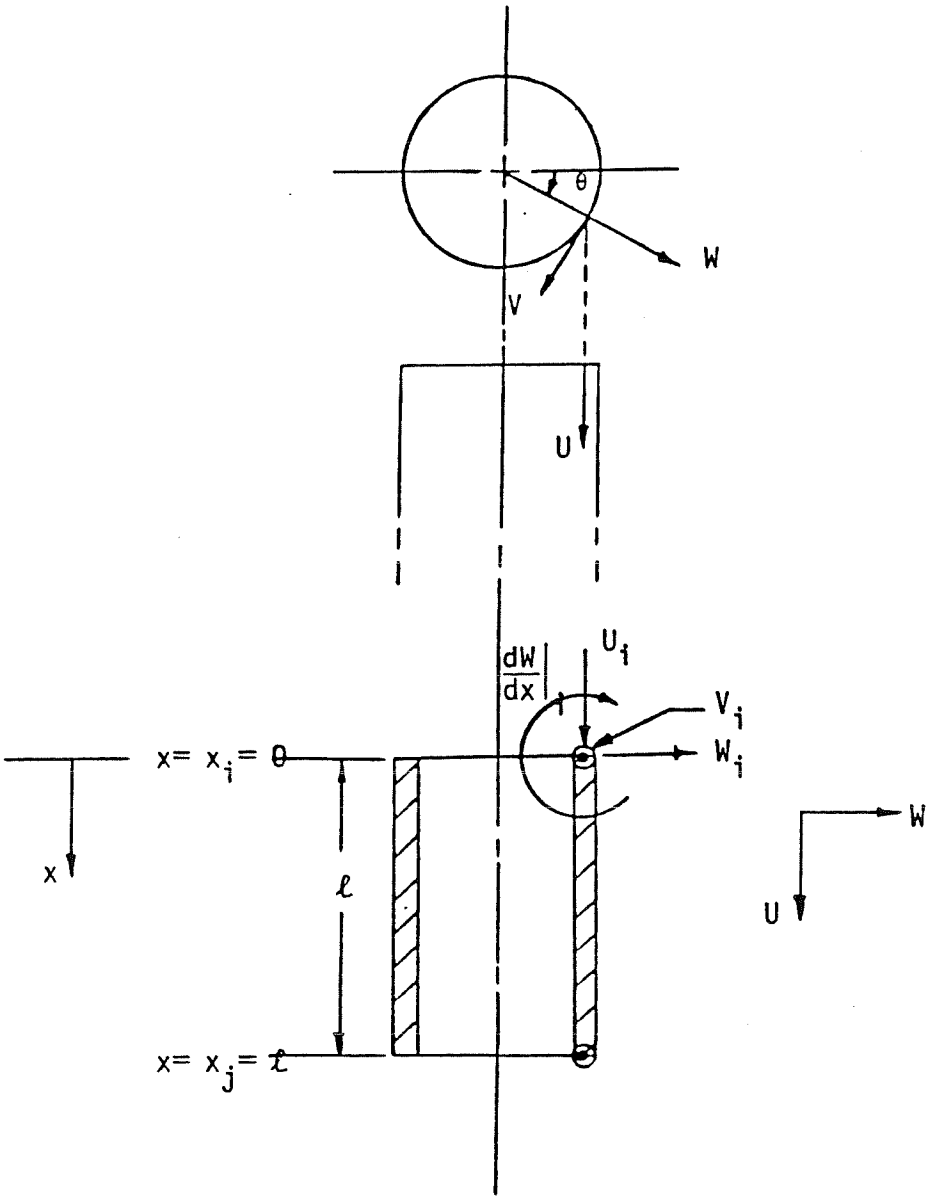

FIGURE 5: Displacements and degrees of freedom at a node

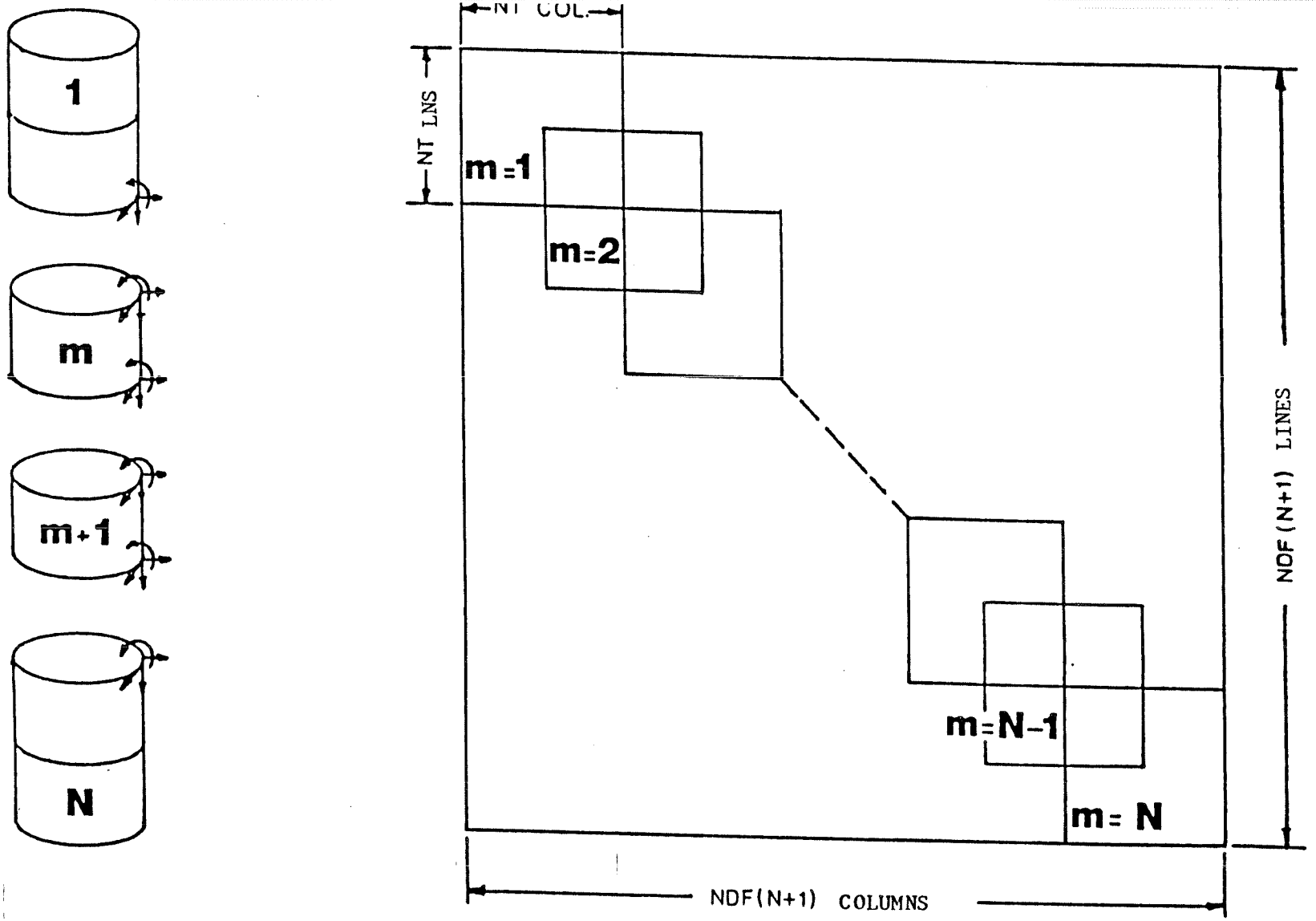

FIGURE 6: Matrix assembly diagram

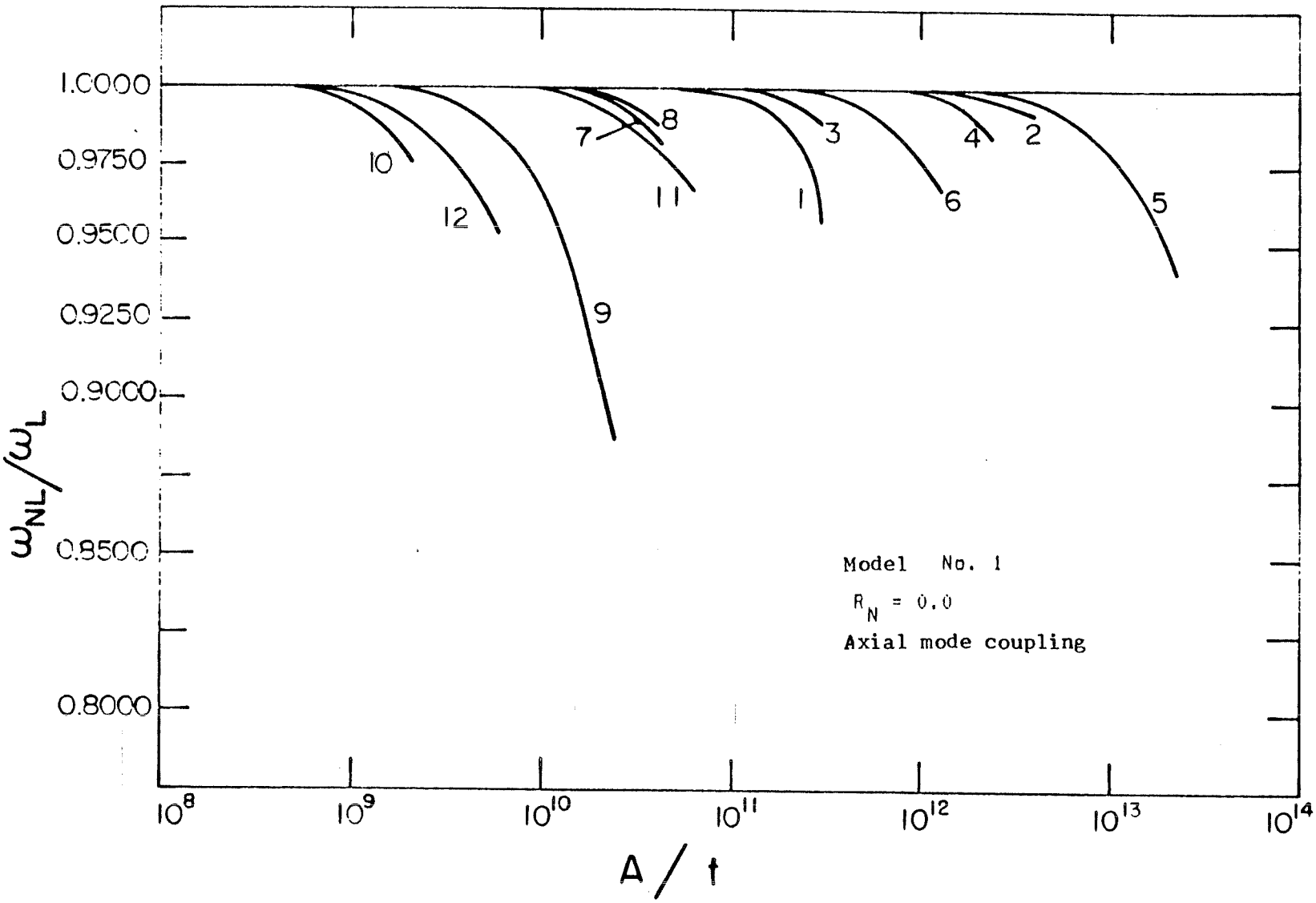

FIGURE 7: Variations in frequency ratio as a function of motion amplitude

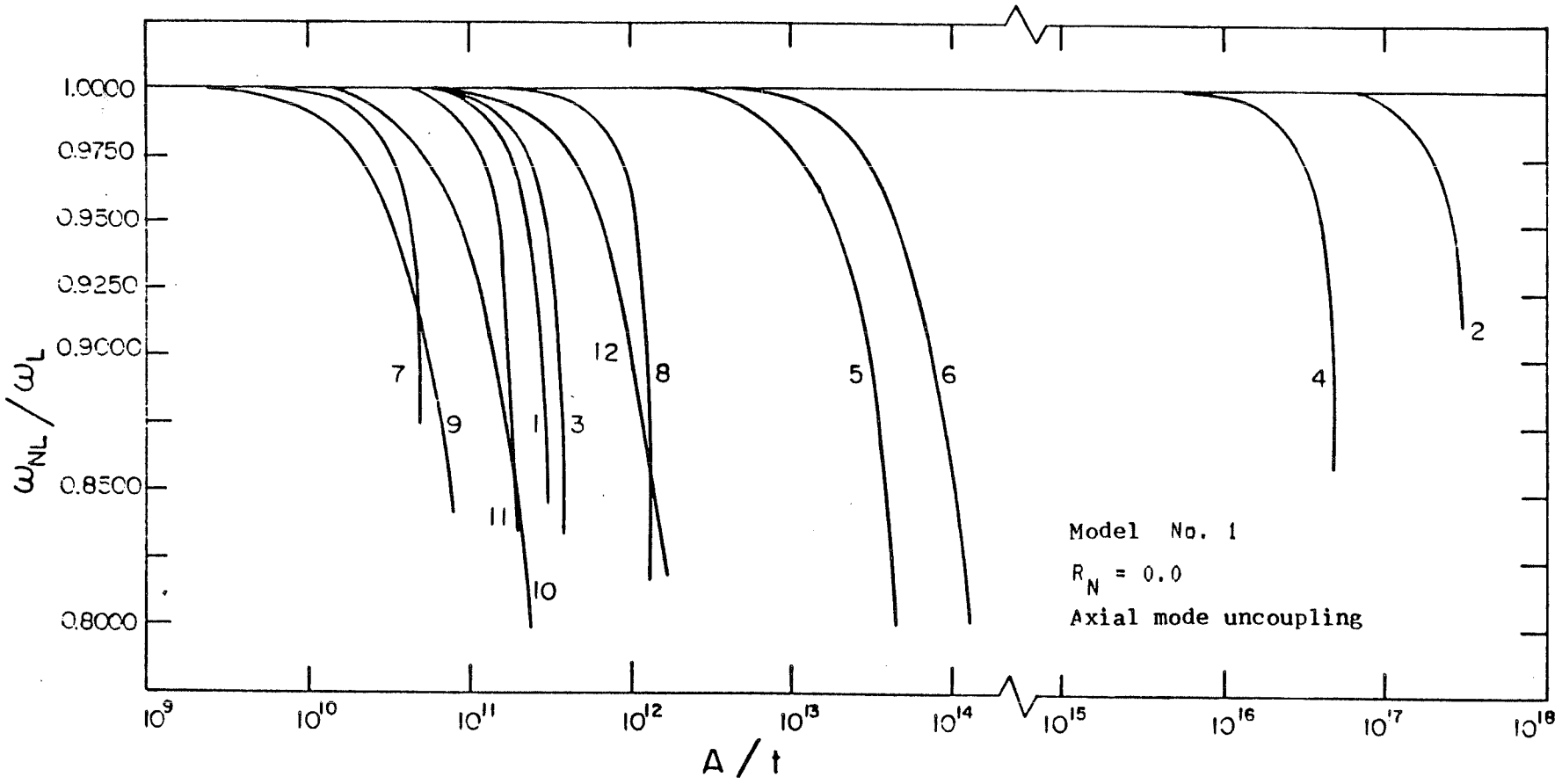

FIGURE 8: Variations in frequency ratio as a function of motion amplitude

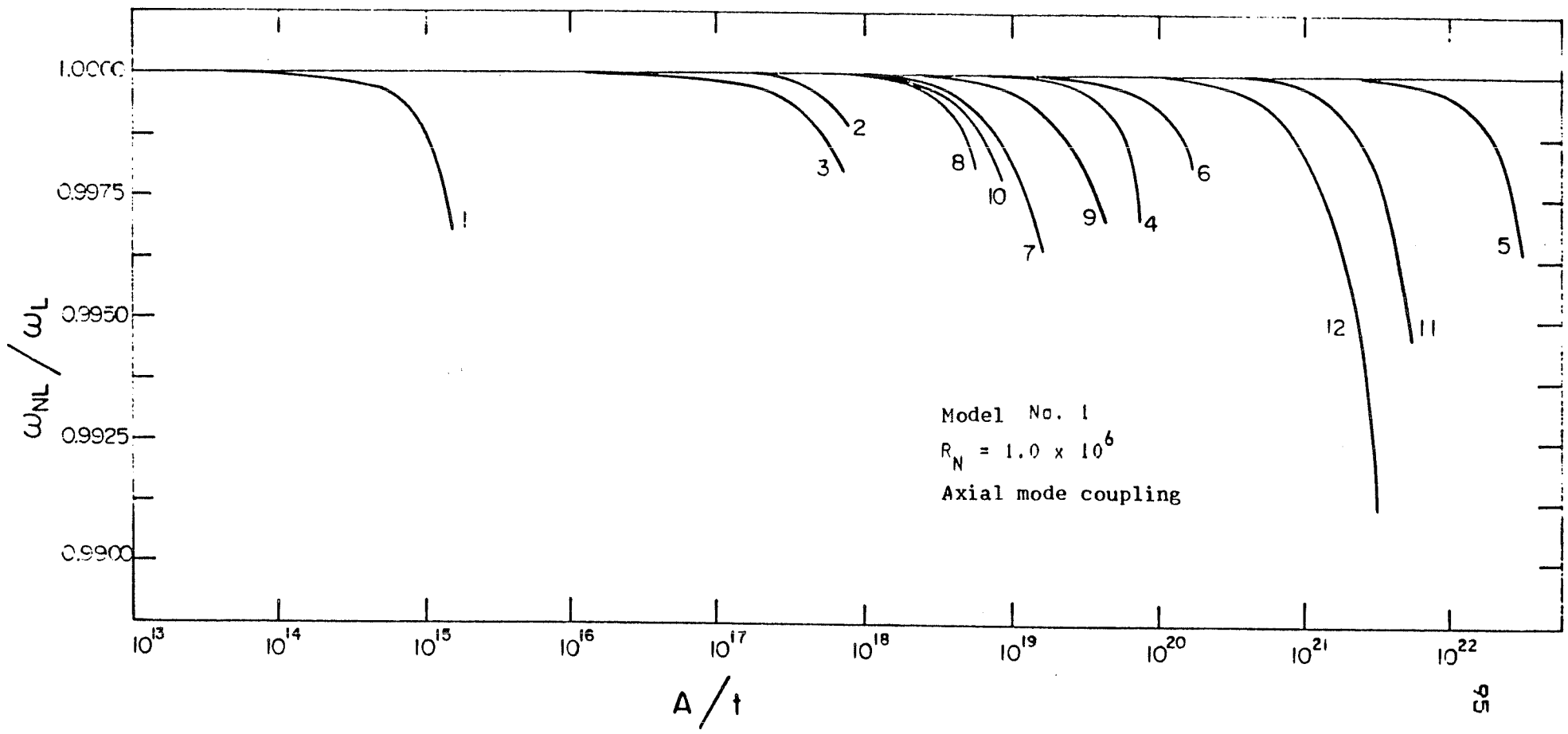

FIGURE 9: Variations in frequency ratio as a function of motion amplitude

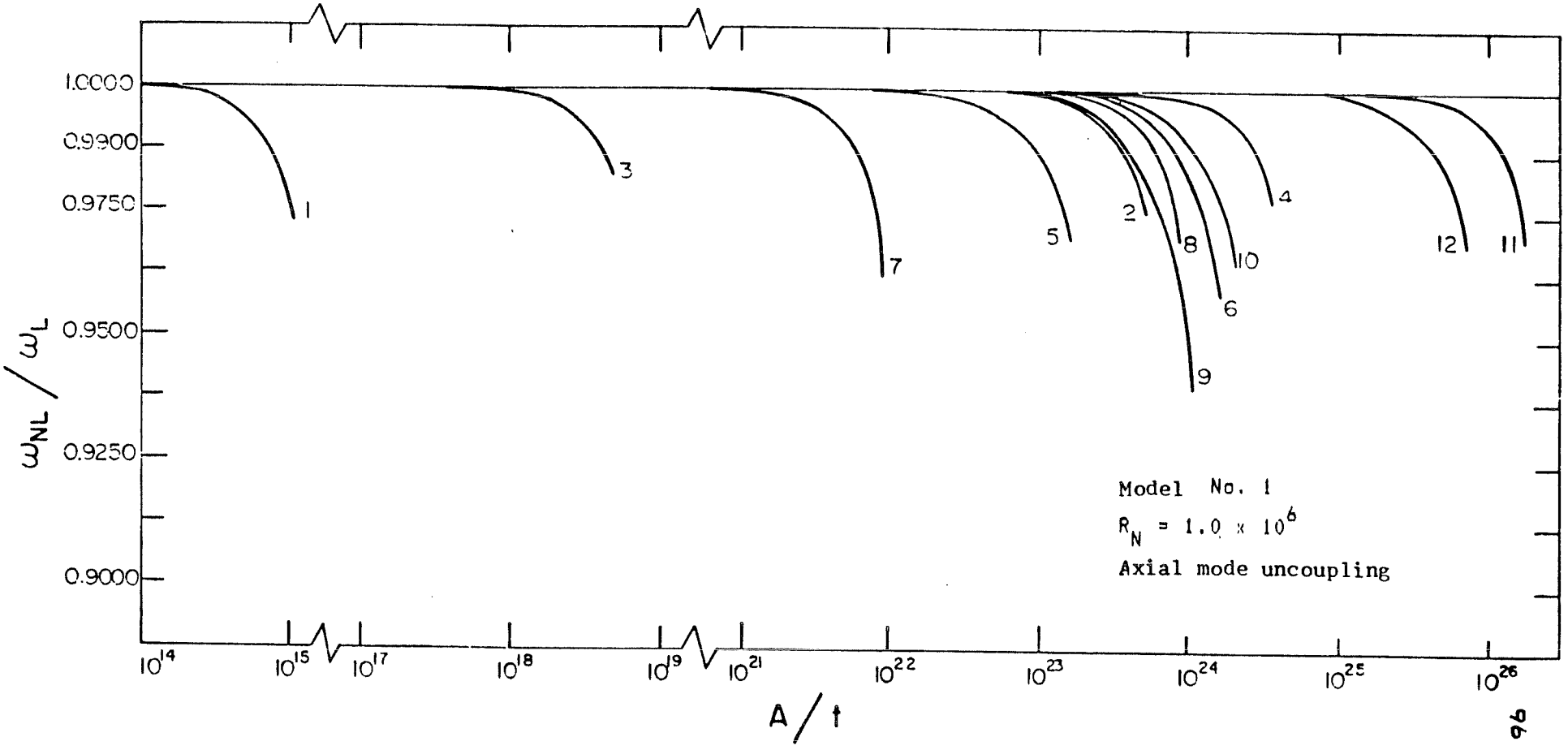

FIGURE 10: Variations in frequency ratio as a function of motion amplitude

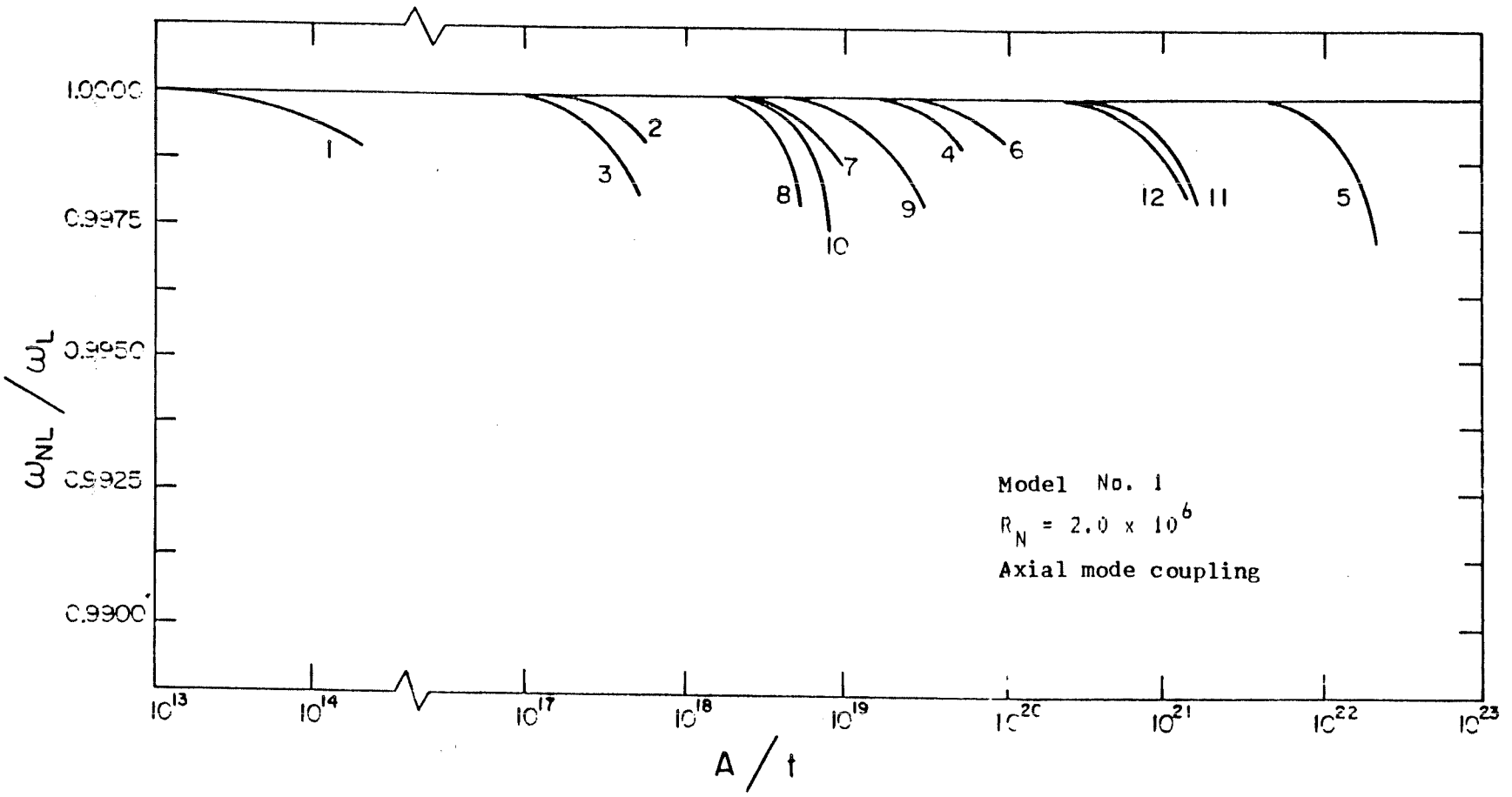

FIGURE 11: Variations in frequency ratio as a function of motion amplitude

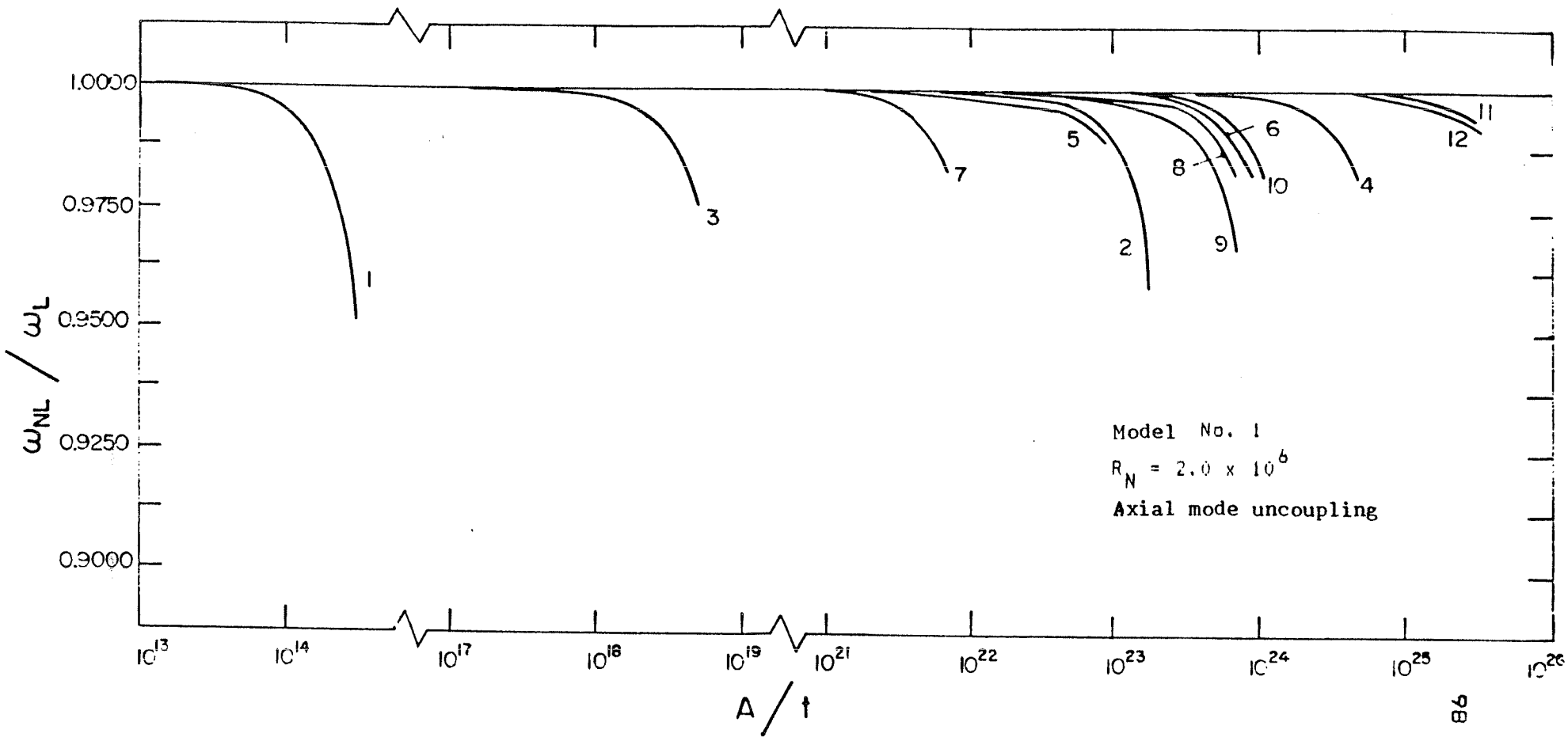

FIGURE 12: Variations in frequency ratio as a function of motion amplitude

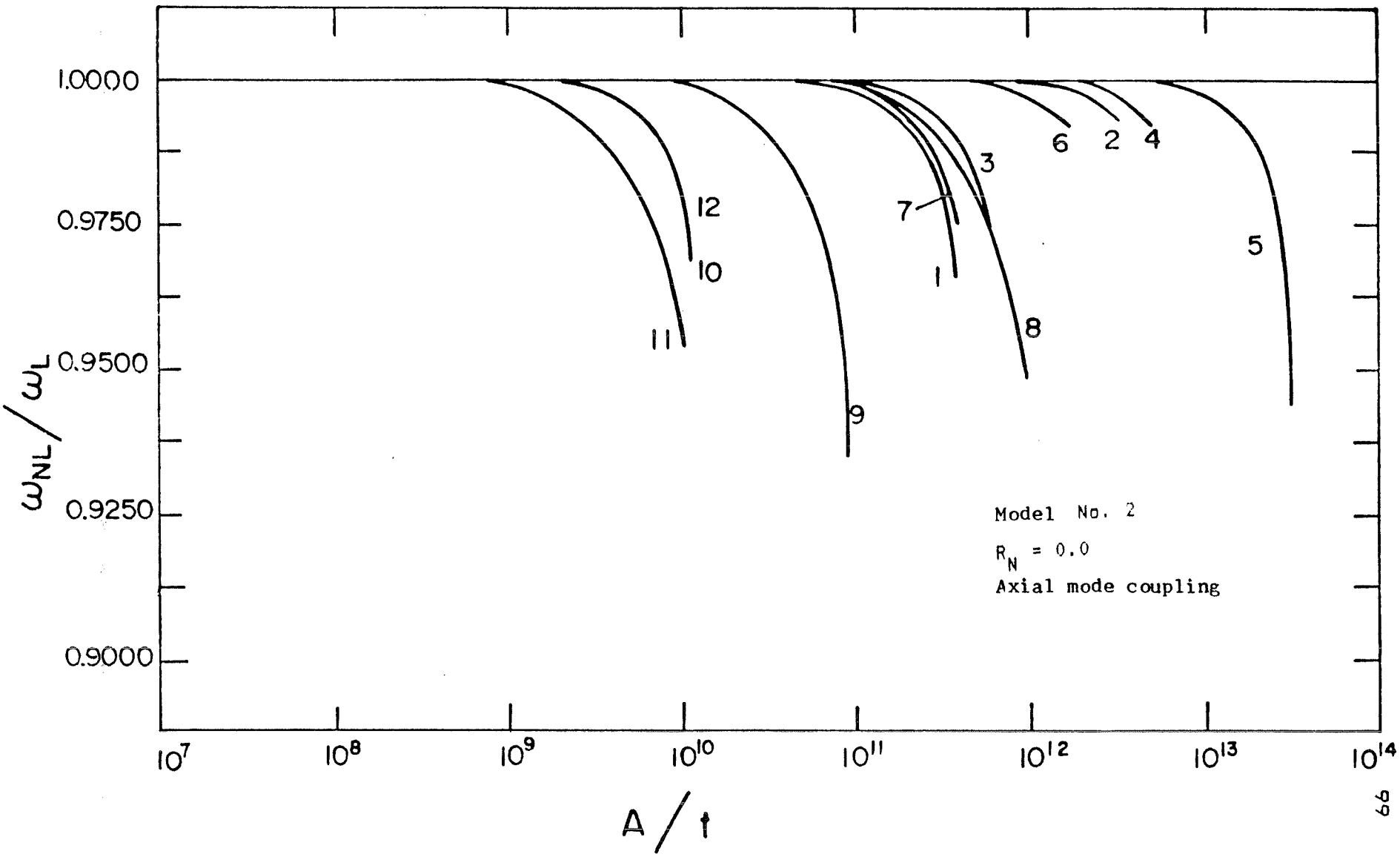

FIGURE 13: Variations in frequency ratio as a function of motion amplitude

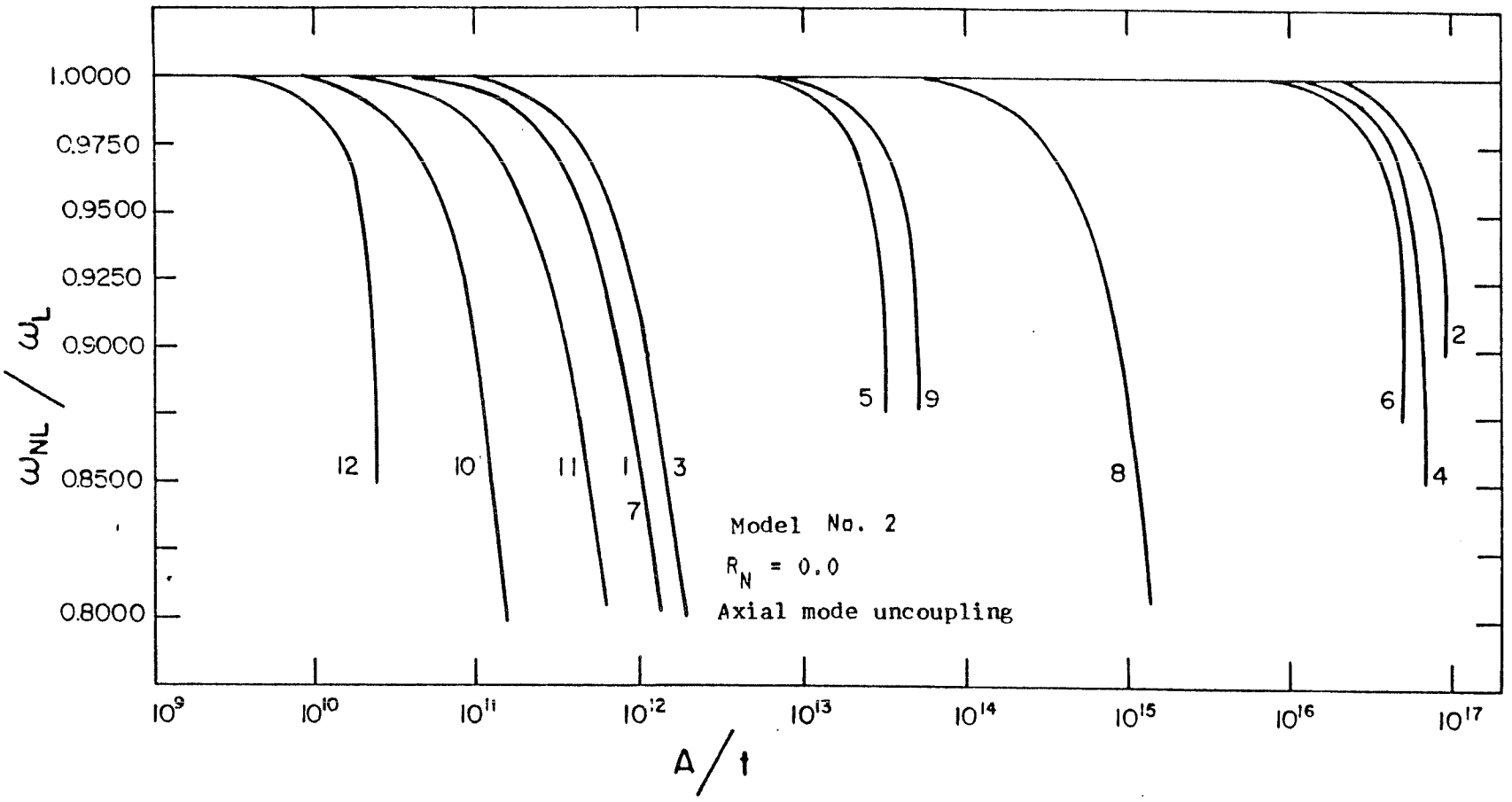

FIGURE 14: Variations in frequency ratio as a function of motion amplitude

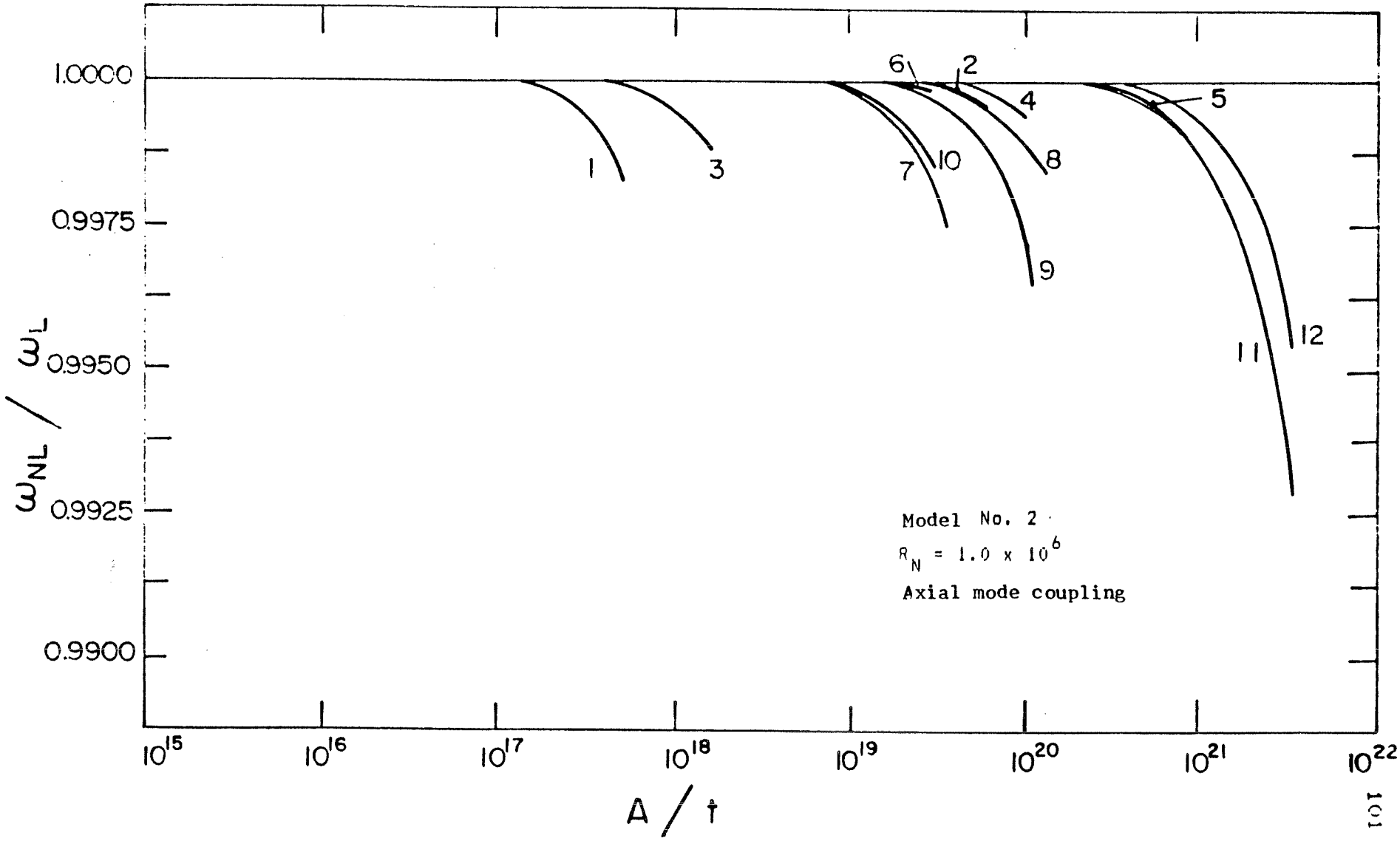

FIGURE 15: Variations in frequency ratio as a function of motion amplitude

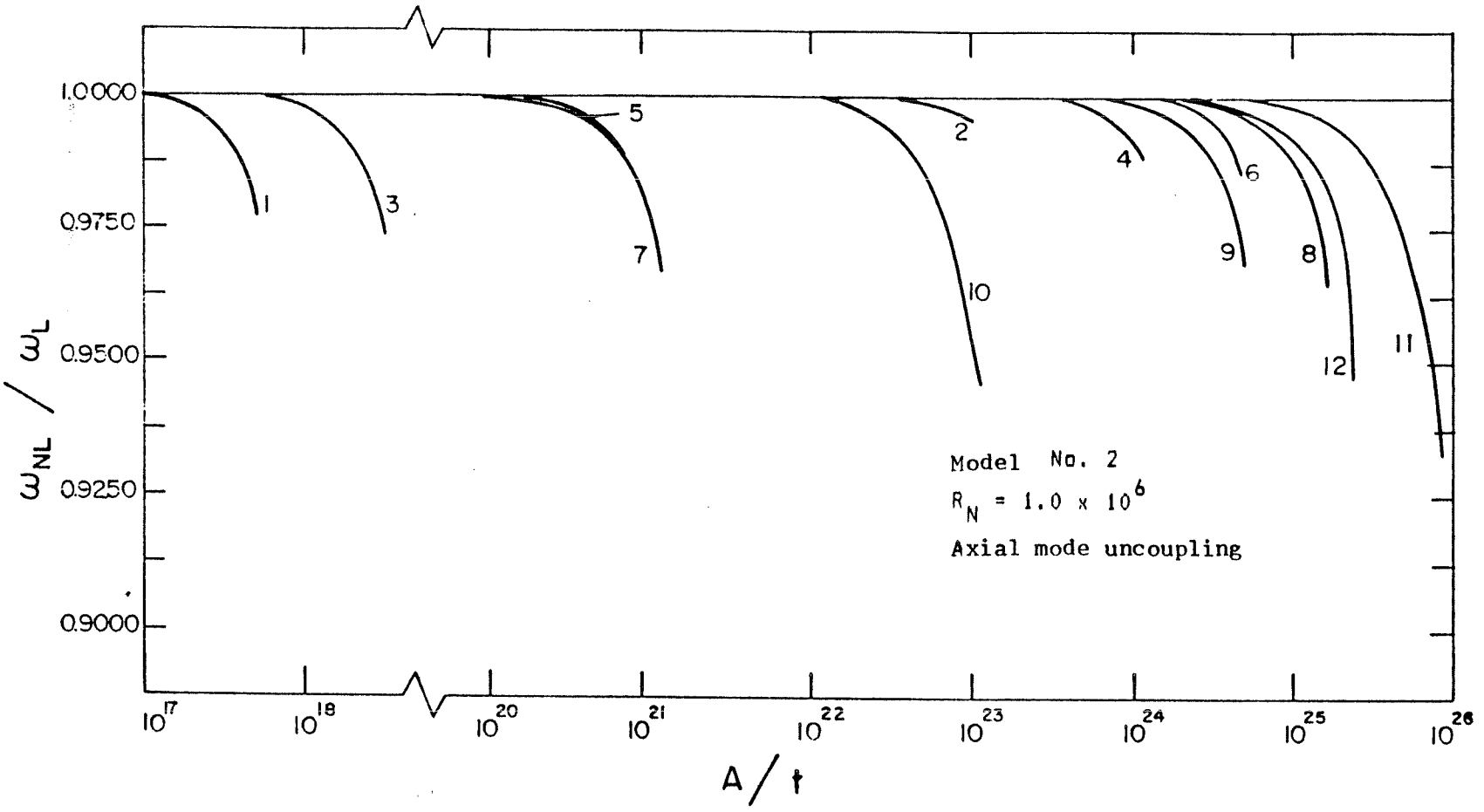

FIGURE 16: Variations in frequency ratio as a function of motion amplitude

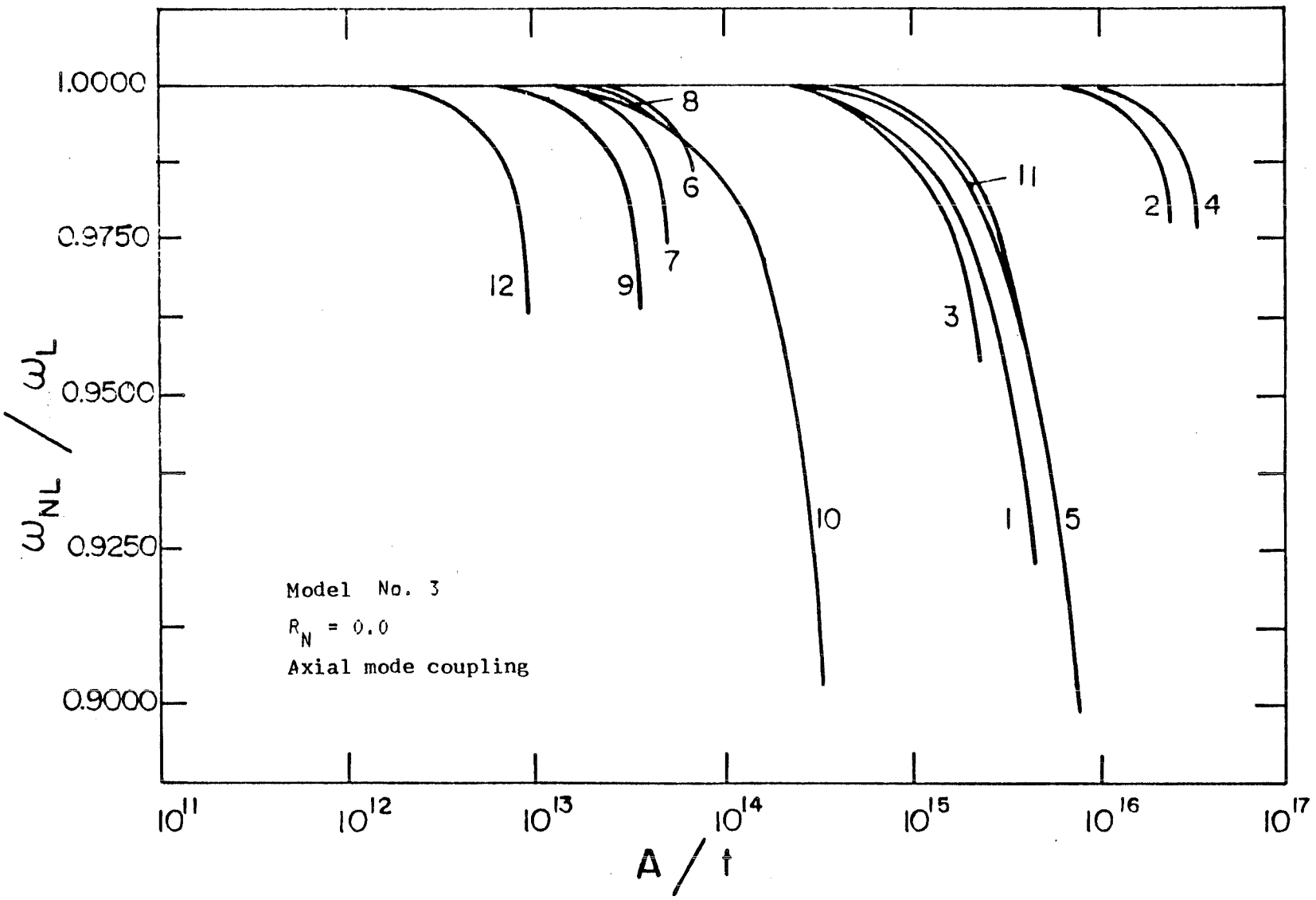

FIGURE 17: Variations in frequency ratio as a function of motion amplitude

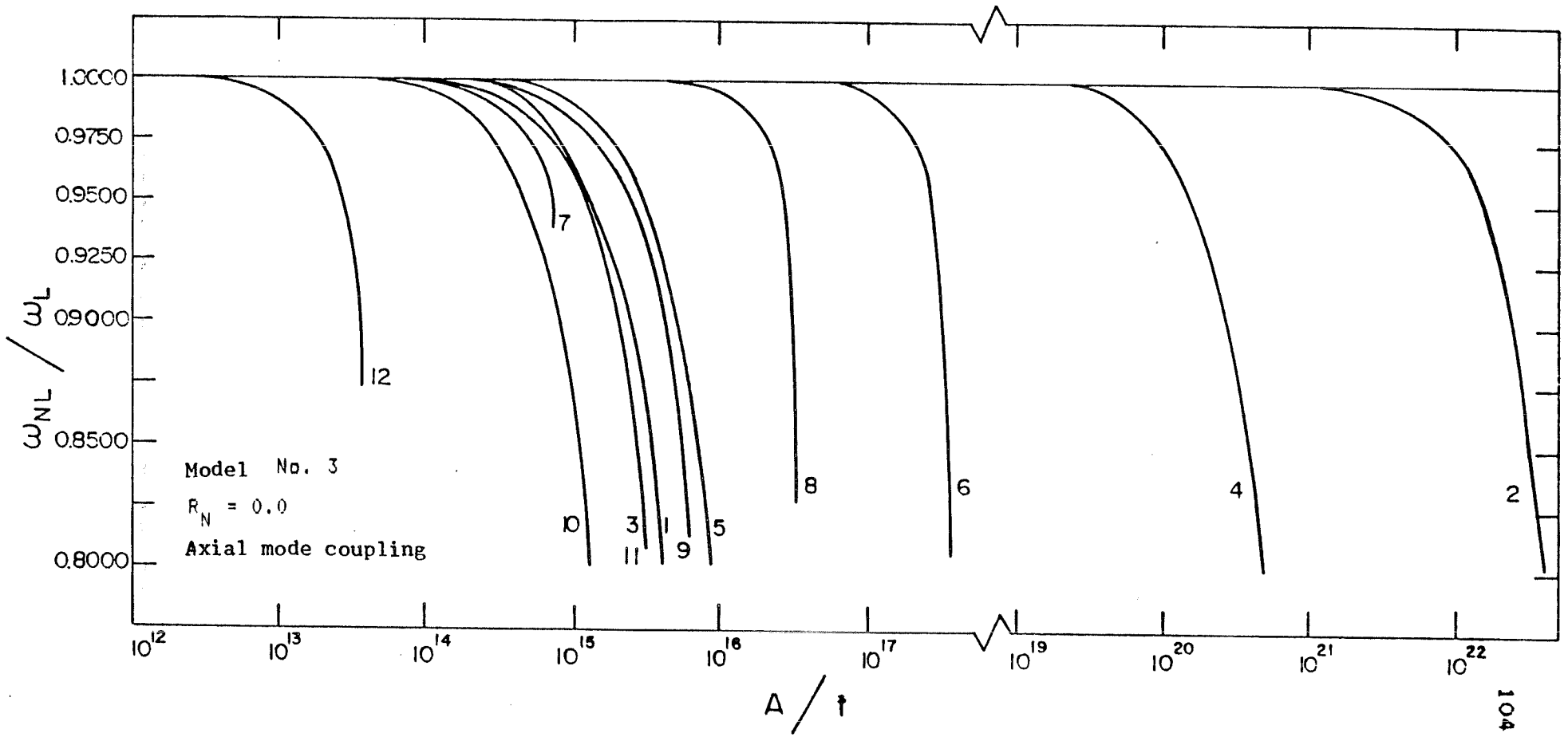

FIGURE 18: Variations in frequency ratio as a function of motion amplitude

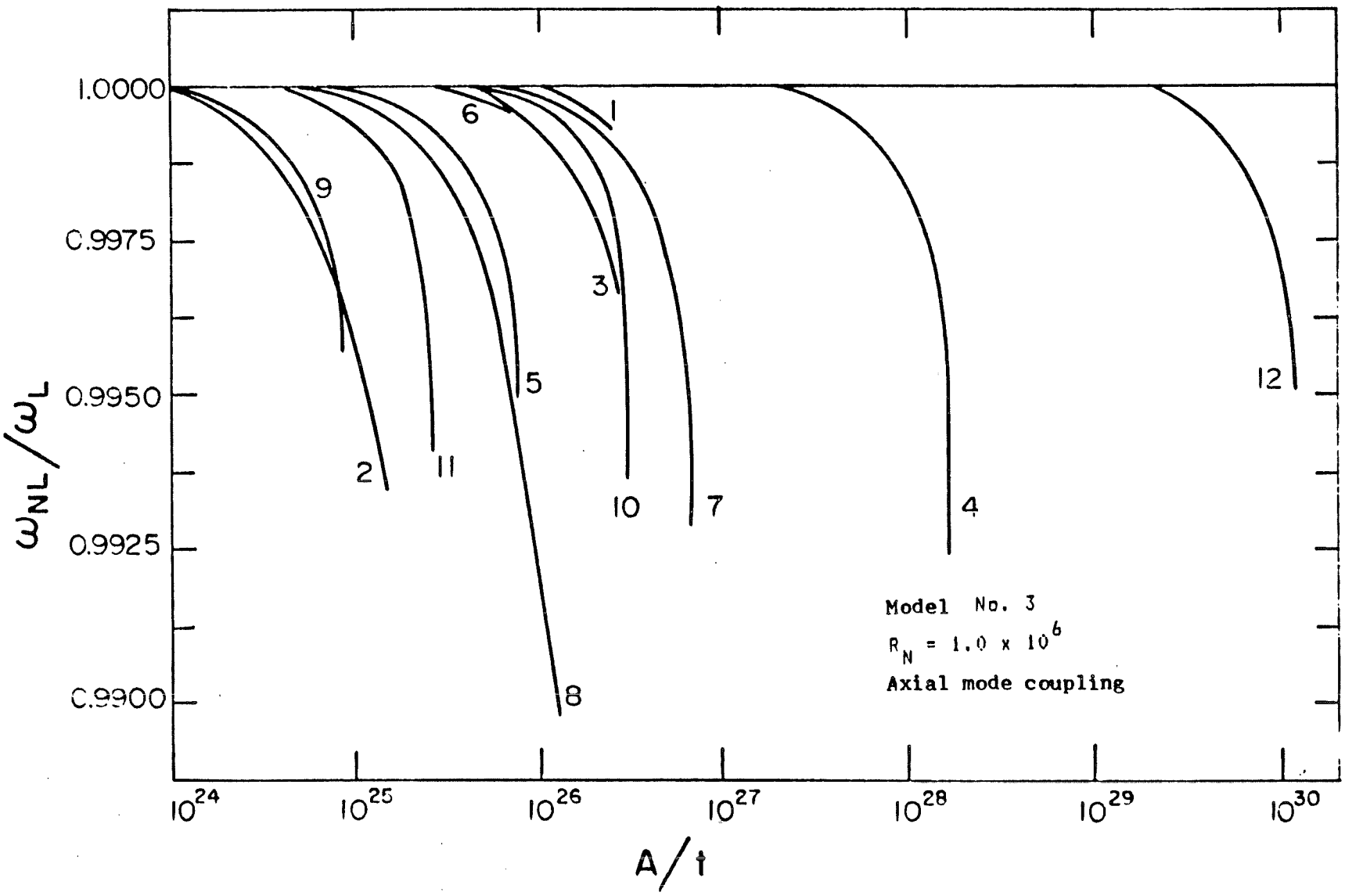

FIGURE 19: Variations in frequency ratio as a function of motion amplitude

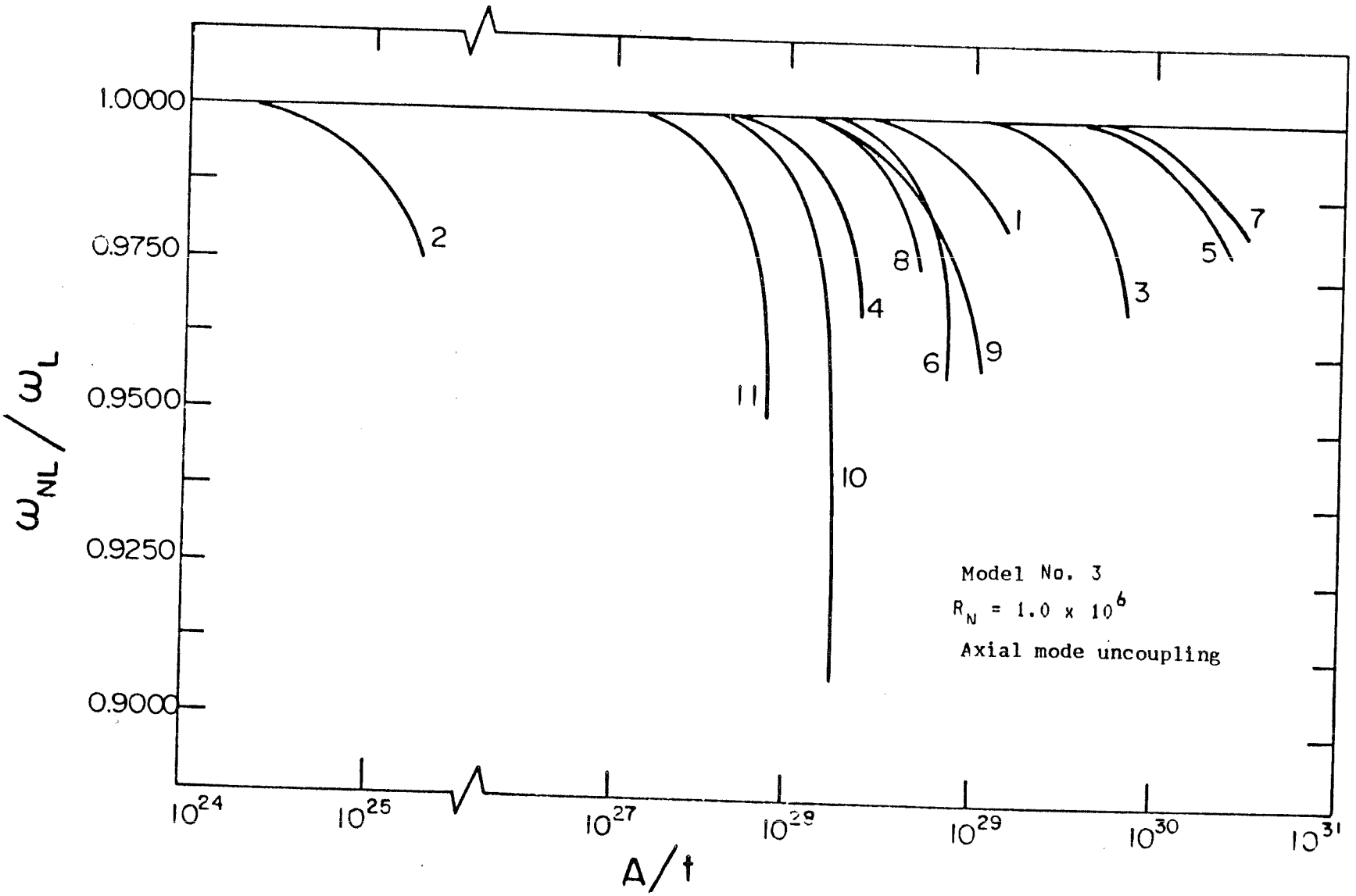

FIGURE 20: Variations in frequency ratio as a function of motion amplitude

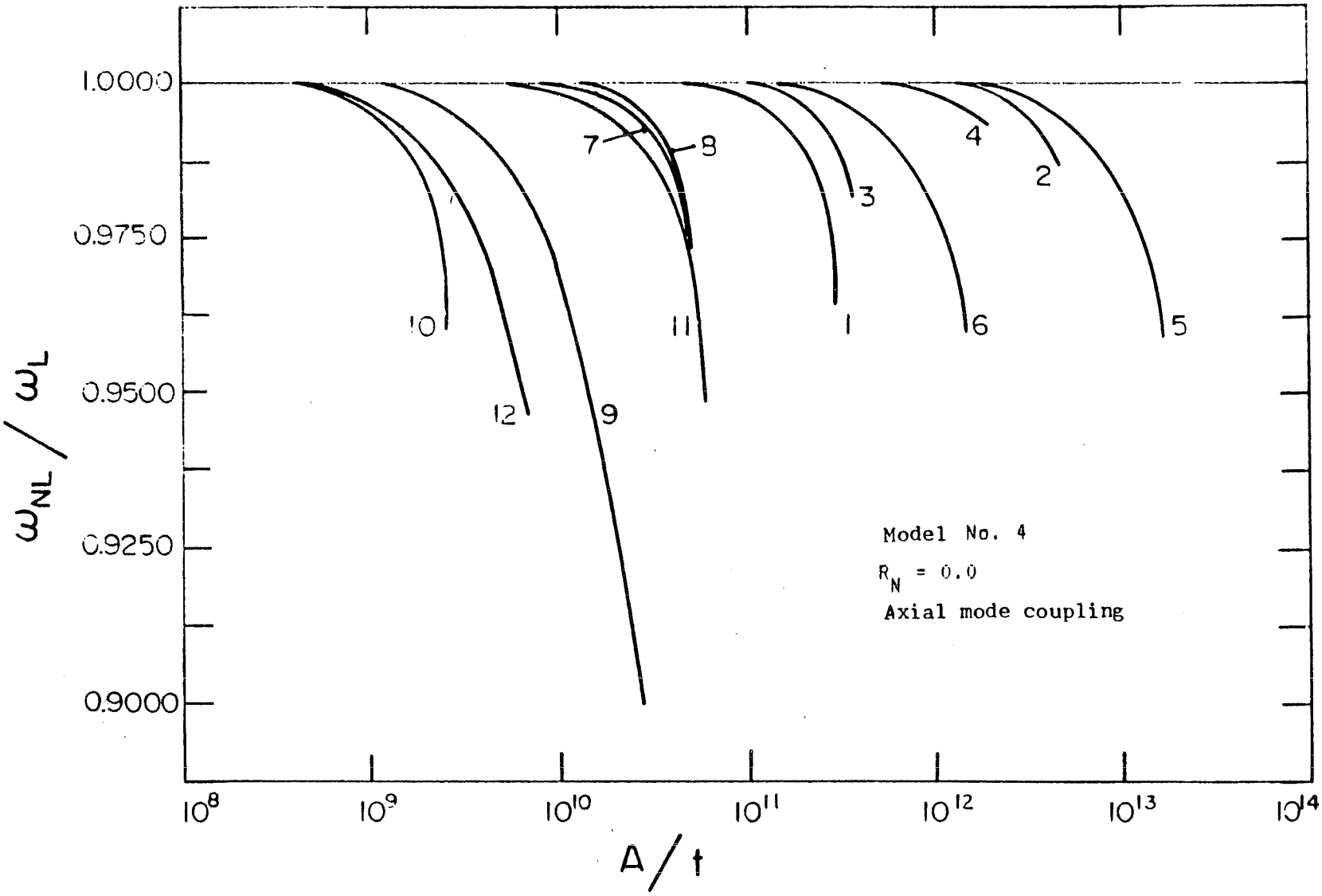

FIGURE 21: Variations in frequency ratio as a function of motion amplitude

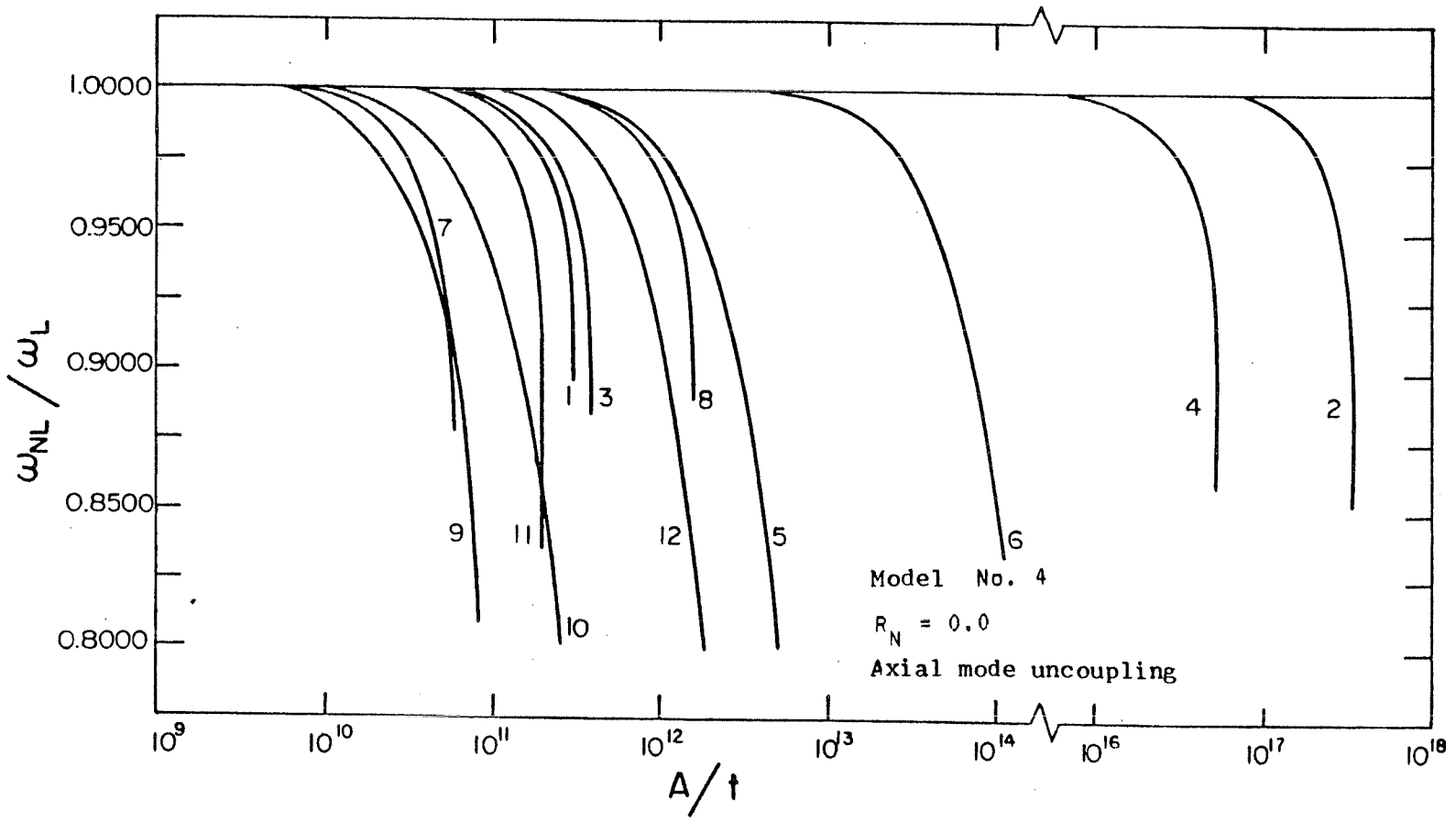

FIGURE 22: Variations in frequency ratio as a function of motion amplitude

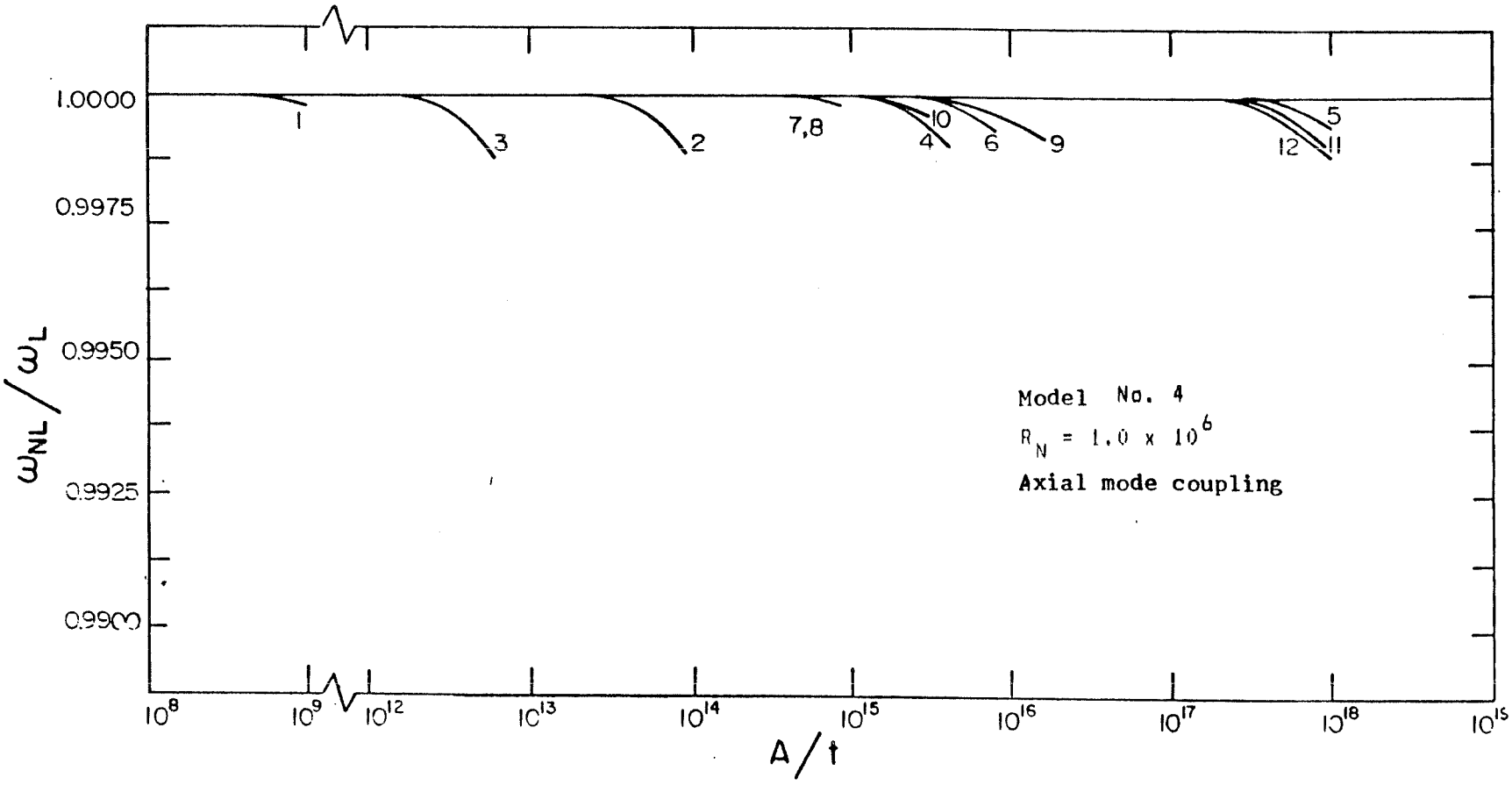

FIGURE 23: Variations in frequency ratio as a function of motion amplitude

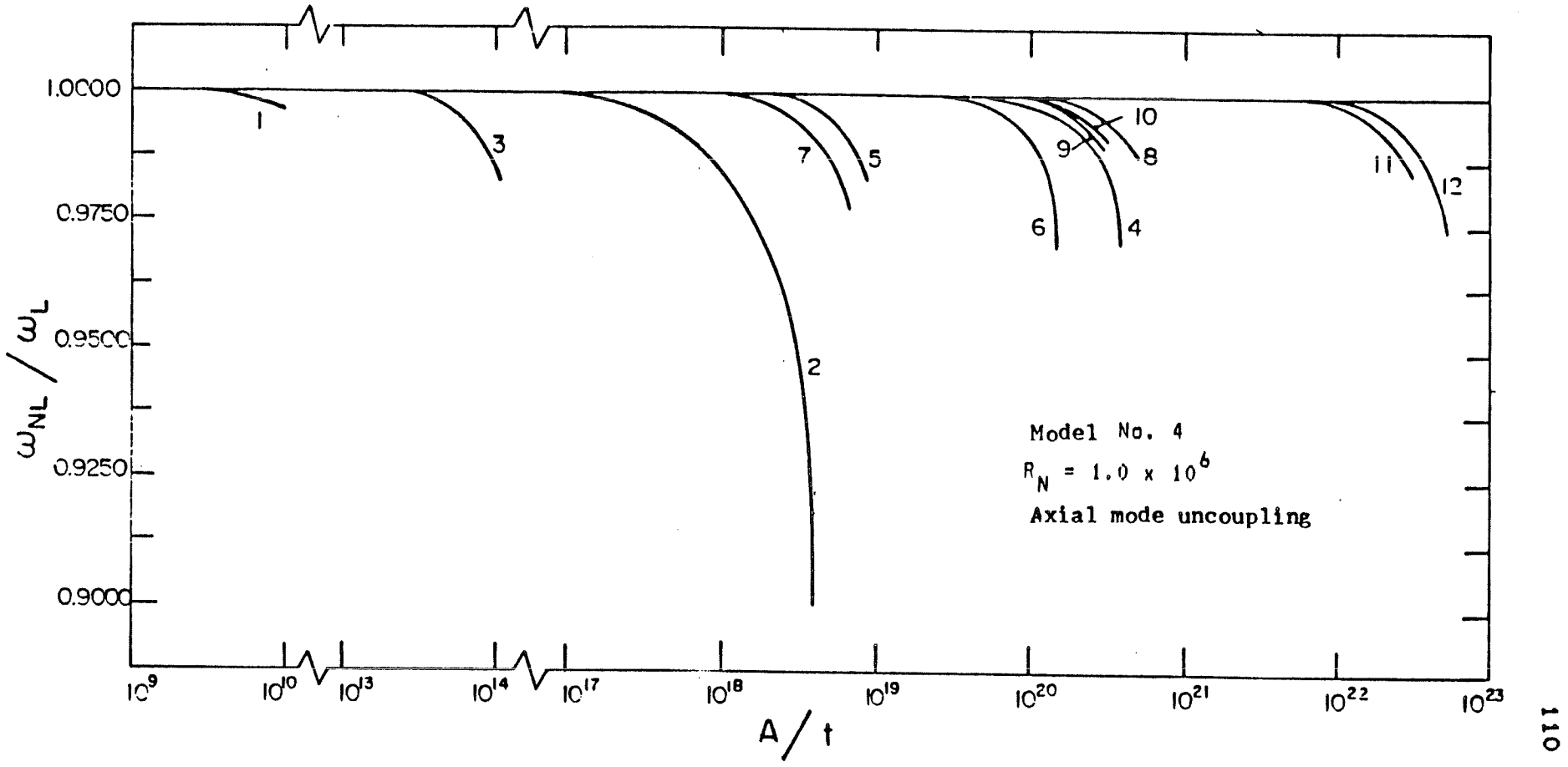

FIGURE 24: Variations in frequency ratio as a function of motion amplitude